

<sup>1</sup> Memory for television episodes preserves event content  
<sup>2</sup> while introducing new across-event similarities

<sup>3</sup> Andrew C. Heusser<sup>1, 2, †</sup>, Paxton C. Fitzpatrick<sup>1, †</sup>, and Jeremy R. Manning<sup>1, \*</sup>

<sup>1</sup>Department of Psychological and Brain Sciences

Dartmouth College, Hanover, NH 03755, USA

<sup>2</sup>Akili Interactive

Boston, MA 02110

<sup>†</sup>Denotes equal contribution

<sup>\*</sup>Corresponding author: jeremy.r.manning@dartmouth.edu

<sup>4</sup> February 13, 2020

<sup>5</sup> **Abstract**

The ways our experiences unfold over time define unique *trajectories* through the relevant representational spaces. Within this geometric framework, one can compare the shape of the trajectory formed by an experience to that defined by our later remembering of that experience. We propose a framework for mapping naturalistic experiences onto geometric spaces that characterize how experiences are segmented into discrete events, and how the contents of event sequences evolve over time. We apply this approach to a naturalistic memory experiment which had participants view and recount a television episode. The content of participants' recounts of events from the original episode closely matched the original episode's content. However, the similarity patterns *across* events was much different in the original episode as compared with participants' recounts. We also identified a network of brain structures that are sensitive to the "shapes" of ongoing experiences, and an overlapping network that is sensitive (at the time

17 of encoding) to how people later remembered those experiences in relation to other experiences.  
18 In this way, modeling the content of richly structured experiences can reveal how (geometrically  
19 and conceptually) those experiences are segmented into events and integrated into our memories  
20 of other experiences.

## 21 **Introduction**

22 What does it mean to *remember* something? In traditional episodic memory experiments (e.g.,  
23 list-learning or trial-based experiments; Murdock, 1962; Kahana, 1996), remembering is often cast  
24 as a discrete and binary operation: each studied item may be separated from all others, and la-  
beled as having been recalled or forgotten. More nuanced studies might incorporate self-reported  
25 confidence measures as a proxy for memory strength, or ask participants to discriminate between  
26 “recollecting” the (contextual) details of an experience or having a general feeling of “familiarity”  
27 (Yonelinas, 2002). Using well-controlled, trial-based experimental designs, the field has amassed  
28 a wealth of valuable information regarding human episodic memory. However, there are funda-  
29 mental properties of the external world and our memories that trial-based experiments are not well  
30 suited to capture (for review also see Kriat and Goldsmith, 1994; Huk et al., 2018). First, our expe-  
31 riences and memories are continuous, rather than discrete—removing a (naturalistic) event from  
32 the context in which it occurs can substantially change its meaning. Second, the specific language  
33 used to describe an experience has little bearing on whether the experience should be considered to  
34 have been “remembered.” Asking whether the rememberer has precisely reproduced a specific set  
35 of words to describe a given experience is nearly orthogonal to whether they were actually able to  
36 remember it. In classic (e.g., list-learning) memory studies, by contrast, the number or proportion  
37 of precise recalls is often a primary metric for assessing the quality of participants’ memories.  
38 Third, one might remember the *essence* (or a general summary) of an experience but forget (or  
39 neglect to recount) particular details. Capturing the essence of what happened is typically the  
40 main “point” of recounting a memory to a listener, while the addition of highly specific details  
41 may add comparatively little to successful conveyance of an experience.  
42

43 How might one go about formally characterizing the “essence” of an experience, or whether  
44 it has been recovered by the rememberer? Any given moment of an experience derives meaning  
45 from surrounding moments, as well as from longer-range temporal associations (Lerner et al.,  
46 2011; Manning, 2019). Therefore, the timecourse describing how an event unfolds is fundamental  
47 to its overall meaning. Further, this hierarchy formed by our subjective experiences at different  
48 timescales defines a *context* for each new moment (e.g., Howard and Kahana, 2002; Howard et al.,  
49 2014), and plays an important role in how we interpret that moment and remember it later (for  
50 review see Manning et al., 2015). Our memory systems can leverage these associations to form  
51 predictions that help guide our behaviors (Ranganath and Ritchey, 2012). For example, as we  
52 navigate the world, the features of our subjective experiences tend to change gradually (e.g., the  
53 room or situation we are in at any given moment is strongly temporally autocorrelated), allowing  
54 us to form stable estimates of our current situation and behave accordingly (Zacks et al., 2007;  
55 Zwaan and Radvansky, 1998).

56 Occasionally, this gradual “drift” of our ongoing experience is punctuated by sudden changes,  
57 or “shifts” (e.g., when we walk through a doorway; Radvansky and Zacks, 2017). Prior research  
58 suggests that these sharp transitions (termed *event boundaries*) help to discretize our experiences  
59 (and their mental representations) into *events* (Radvansky and Zacks, 2017; Brunec et al., 2018;  
60 Heusser et al., 2018a; Clewett and Davachi, 2017; Ezzyat and Davachi, 2011; DuBrow and Davachi,  
61 2013). The interplay between the stable (within-event) and transient (across-event) temporal  
62 dynamics of an experience also provides a potential framework for transforming experiences into  
63 memories that distill those experiences down to their essence. For example, prior work has shown  
64 that event boundaries can influence how we learn sequences of items (Heusser et al., 2018a; DuBrow  
65 and Davachi, 2013), navigate (Brunec et al., 2018), and remember and understand narratives (Zwaan  
66 and Radvansky, 1998; Ezzyat and Davachi, 2011). Prior research has implicated the hippocampus  
67 and the medial prefrontal cortex as playing a critical role in transforming experiences into structured  
68 and consolidated memories (Tompry and Davachi, 2017).

69 Here we sought to examine how the temporal dynamics of a “naturalistic” experience were  
70 later reflected in participants’ memories. We analyzed an open dataset that comprised behavioral

71 and functional Magnetic Resonance Imaging (fMRI) data collected as participants viewed and then  
72 verbally recounted an episode of the BBC television series *Sherlock* (Chen et al., 2017). We developed  
73 a computational framework for characterizing the temporal dynamics of the moment-by-moment  
74 content of the episode, and of participants' verbal recalls. Specifically, we use topic modeling (Blei  
75 et al., 2003) to characterize the thematic conceptual (semantic) content present in each moment of  
76 the episode and recalls, and Hidden Markov Models (Rabiner, 1989; Baldassano et al., 2017) to  
77 discretize this evolving semantic content into events. In this way, we cast naturalistic experiences  
78 (and recalls of those experiences) as geometric *trajectories* that describe how the experiences evolve  
79 over time. Under this framework, successful remembering entails verbally "traversing" the content  
80 trajectory of the episode, thereby reproducing the shape (or essence) of the original experience.  
81 Comparing the shapes of the topic trajectories of the episode and of participants' retellings of  
82 the episode then reveals which aspects of the episode were preserved (or lost) in the translation  
83 into memory. We further introduce two novel metrics for assessing memory quality: the *precision*  
84 with which a participant recounts each event and 2) the *distinctiveness* of each recall event (relative  
85 to other recalled events). We examine how these metrics relate to participants' overall memory  
86 performance, and discuss the ways in which they improve upon classic "proportion-recalled"  
87 measures for analyzing naturalistic memory. Last, we utilize our framework to identify networks  
88 of brain structures whose responses (as participants watched the episode) reflected the temporal  
89 dynamics of the episode, and how participants would later recount it.

## 90 Results

91 To characterize the "essence" of the *Sherlock* episode and participants' subsequent recounts of  
92 its unfolding, we used a topic model (Blei et al., 2003) to discover the latent themes in the episode's  
93 dynamic content. Topic models take as inputs a vocabulary of words to consider and a collection  
94 of text documents, and return two output matrices. The first of these is a *topics matrix* whose rows  
95 are topics (latent themes) and whose columns correspond to words in the vocabulary. The entries  
96 of the topics matrix define how each word in the vocabulary is weighted by each discovered topic.

97 For example, a detective-themed topic might weight heavily on words like “crime,” and “search.”  
98 The second output is a *topic proportions matrix*, with one row per document and one column per  
99 topic. The topic proportions matrix describes what mixture of discovered topics is reflected in each  
100 document.

101 Chen et al. (2017) collected hand-annotated information about each of 1000 (manually identified)  
102 time segments spanning the roughly 50 minute video used in their experiment. This information  
103 included: a brief narrative description of what was happening, the location where the scene  
104 took place, the names of any characters on the screen, and other similar details (for a full list of  
105 annotated features, see *Methods*). We took from these annotations the union of all unique words  
106 (excluding stop words, such as “and,” “or,” “but,” etc.) across all features and scenes as the  
107 “vocabulary” for the topic model. We then concatenated the sets of words across all features  
108 contained in overlapping, sliding windows of (up to) 50 scenes, and treated each window as a  
109 single “document” for the purpose of fitting the topic model. Next, we fit a topic model with (up  
110 to)  $K = 100$  topics to this collection of documents. We found that 32 unique topics (with non-zero  
111 weights) were sufficient to describe the time-varying content of the video (see *Methods*; Figs. 1, S2).  
112 Note that our approach is similar in some respects to Dynamic Topic Models (Blei and Lafferty,  
113 2006) in that we sought to characterize how the thematic content of the episode evolved over  
114 time. However, whereas Dynamic Topic Models are designed to characterize how the properties  
115 of *collections* of documents change over time, our sliding window approach allows us to examine  
116 the topic dynamics within a single document (or video). Specifically, our approach yielded (via the  
117 topic proportions matrix) a single *topic vector* for each sliding window of annotations transformed  
118 by the topic model. We then stretched the resulting windows-by-topics matrix to match the time  
119 series of the 1976 fMRI volumes collected as participants viewed the episode.

120 The 32 topics we found were heavily character-focused (i.e., the top-weighted word in each  
121 topic was nearly always a character) and could be roughly divided into themes centered around  
122 Sherlock Holmes (the titular character), John Watson (Sherlock’s close confidant and assistant),  
123 supporting characters (e.g., Inspector Lestrade, Sergeant Donovan, or Sherlock’s brother Mycroft),  
124 or the interactions between various pairs of these characters (see Fig. S2). Several of the identified

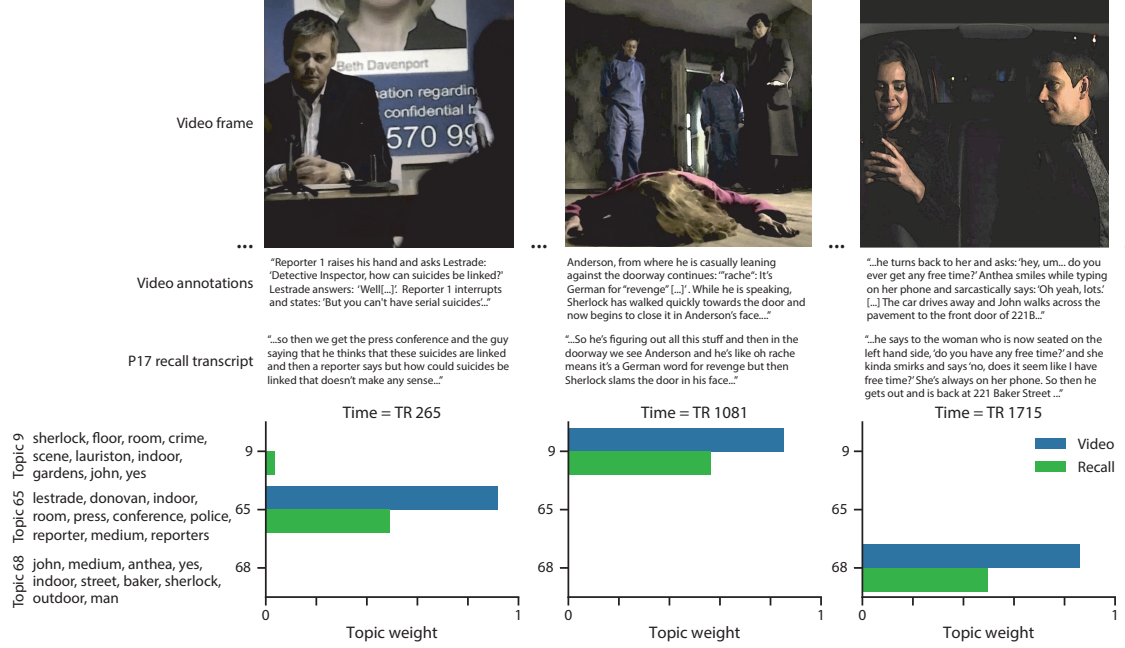


**Figure 1: Methods overview.** We used hand-annotated descriptions of each moment of video to fit a topic model. Three example video frames and their associated descriptions are displayed (top two rows). Participants later recalled the video (in the third row, we show example recalls of the same three scenes from participant 13). We used the topic model (fit to the annotations) to estimate topic vectors for each moment of video and each sentence the participants recalled. Example topic vectors are displayed in the bottom row (blue: video annotations; green: example participant’s recalls). Three topic dimensions are shown (the highest-weighted topics for each of the three example scenes, respectively). We also show the 10 highest-weighted words for each topic. Figure S2 provides a full list of the top 10 words from each of the discovered topics.

125 topics were highly similar, which we hypothesized might allow us to distinguish between subtle  
126 narrative differences if the distinctions between those overlapping topics were meaningful. The  
127 topic vectors for each timepoint were *sparse*, in that only a small number (usually one or two) of  
128 topics tended to be “active” in any given timepoint (Fig. 2A). Further, the dynamics of the topic  
129 activations appeared to exhibit *persistence* (i.e., given that a topic was active in one timepoint, it was  
130 likely to be active in the following timepoint) along with *occasional rapid changes* (i.e., occasionally  
131 topics would appear to spring into or out of existence). These two properties of the topic dynamics  
132 may be seen in the block diagonal structure of the timepoint-by-timepoint correlation matrix  
133 (Fig. 2B) and reflect the gradual drift and sudden shifts fundamental to the temporal dynamics of  
134 real-world experiences. Given this observation, we adapted an approach devised by Baldassano  
135 et al. (2017), and used a Hidden Markov Model (HMM) to identify the *event boundaries* where the  
136 topic activations changed rapidly (i.e., at the boundaries of the blocks in the correlation matrix;  
137 event boundaries identified by the HMM are outlined in yellow in Fig. 2B). Part of our model fitting  
138 procedure required selecting an appropriate number of “events” into which the topic trajectory  
139 should be segmented. To accomplish this, we used an optimization procedure that maximized the  
140 difference between the topic weights for timepoints within an event and across multiple events  
141 (see *Methods* for additional details). We then created a stable “summary” of the content within  
142 each video event by averaging the topic vectors across timepoints each event spanned (Fig. 2C).

143 Given that the time-varying content of the video could be segmented cleanly into discrete  
144 events, we wondered whether participants’ recalls of the video also displayed a similar structure.  
145 We applied the same topic model (already trained on the video annotations) to each participant’s  
146 recalls. Analogous to how we parsed the time-varying content of the video, to obtain similar esti-  
147 mates for each participant’s recall, we treated each overlapping “window” of (up to 10) sentences  
148 from their transcript as a “document,” and computed the most probable mix of topics reflected in  
149 each timepoint’s sentences. This yielded, for each participant, a number-of-windows by number-  
150 of-topics topic proportions matrix that characterized how the topics identified in the original video  
151 were reflected in the participant’s recalls. Note that an important feature of our approach is that it  
152 allows us to compare participants’ recalls to events from the original video, despite different par-



**Figure 2: Modelling naturalistic stimuli and recalls.** All panels: darker colors indicate greater values; range: [0, 1]. **A.** Topic vectors ( $K = 100$ ) for each of the 1976 video timepoints. **B.** Timepoint-by-timepoint correlation matrix of the topic vectors displayed in Panel A. Event boundaries discovered by the HMM are denoted in yellow (30 events detected). **C.** Average topic vectors for each of the 30 video events. **D.** Topic vectors for each of 265 sliding windows of sentences spoken by an example participant while recalling the video. **E.** Timepoint-by-timepoint correlation matrix of the topic vectors displayed in Panel D. Event boundaries detected by the HMM are denoted in yellow (22 events detected). For similar plots for all participants see Figure S4. **F.** Average topic vectors for each of the 22 recalled events from the example participant. **G.** Correlations between the topic vectors for every pair of video events (Panel C) and recalled events (from the example participant; Panel F). For similar plots for all participants, see Figure S5. **H.** Average correlations between each pair of video events and recalled events (across all 17 participants). To create the figure, each recalled event was assigned to the video event with the most correlated topic vector (yellow boxes in panels G and H). The heat maps in each panel were created using Seaborn (Waskom et al., 2016).

153 participants using widely varying language to describe the same event, and that those descriptions  
154 may not match the original annotations. This is a substantial benefit of projecting the video and  
155 recalls into a shared “topic” space. An example topic proportions matrix from one participant’s  
156 recalls is shown in Figure 2D.

157 Although the example participant’s recall topic proportions matrix has some visual similarity to  
158 the video topic proportions matrix, the time-varying topic proportions for the example participant’s  
159 recalls are not as sparse as those for the video (compare Figs. 2A and D). Similarly, although there do  
160 appear to be periods of stability in the recall topic dynamics (i.e., most topics are active or inactive  
161 over contiguous blocks of time), the individual topics’ overall timecourses are not as cleanly  
162 delineated as the video topics’. To examine these patterns in detail, we computed the timepoint-  
163 by-timepoint correlation matrix for the example participant’s recall topic trajectory (Fig. 2E). As  
164 in the video correlation matrix (Fig. 2B), the example participant’s recall correlation matrix has a  
165 strong block diagonal structure, indicating that their recalls are discretized into separated events.  
166 As for the video correlation matrix, we can use an HMM, along with the aforementioned number-  
167 of-events optimization procedure (also see *Methods*) to determine how many events are reflected  
168 in the participant’s recalls and where specifically the event boundaries fall (outlined in yellow).  
169 We carried out a similar analysis on all 17 participants’ recall topic proportions matrices (Fig. S4).

170 Two clear patterns emerged from this set of analyses. First, although every individual partic-  
171 ipant’s recalls could be segmented into discrete events (i.e., every individual participant’s recall  
172 correlation matrix exhibited clear block diagonal structure; Fig. S4), each participant appeared to  
173 have a unique *recall resolution*, reflected in the sizes of those blocks. While, some participants’ recall  
174 topic proportions segmented into just a few events (e.g., Participants P4, P5, and P7), others’ seg-  
175 mented into many shorter duration events (e.g., Participants P12, P13, and P17). This suggests that  
176 different participants may be recalling the video with different levels of detail— e.g., some might  
177 touch on just the major plot points, whereas others might attempt to recall every minor scene or ac-  
178 tion. The second clear pattern present in every individual participant’s recall correlation matrix is  
179 that, unlike in the video correlation matrix, there are substantial off-diagonal correlations. Whereas  
180 each event in the original video was (largely) separable from the others (Fig. 2B), in transforming

<sup>181</sup> those separable events into memory, participants appear to be integrating across multiple events,  
<sup>182</sup> blending elements of previously recalled and not-yet-recalled content into each newly recalled  
<sup>183</sup> event (Figs. 2D, S4; also see Manning et al., 2011; Howard et al., 2012).

<sup>184</sup> The above results indicate that both the structure of the original video and participants' recalls  
<sup>185</sup> of the video exhibit event boundaries that can be identified automatically by characterizing the  
<sup>186</sup> dynamic content using a shared topic model and segmenting the content into events via HMMs.  
<sup>187</sup> Next, we asked whether some correspondence might be made between the specific content of the  
<sup>188</sup> events the participants experienced in the video, and the events they later recalled. One approach  
<sup>189</sup> to linking the experienced (video) and recalled events is to label each recalled event as matching  
<sup>190</sup> the video event with the most similar (i.e., most highly correlated) topic vector (Figs. 2G, S5). This  
<sup>191</sup> yields a sequence of "presented" events from the original video, and a (potentially differently  
<sup>192</sup> ordered) sequence of "recalled" events for each participant. Analogous to classic list-learning  
<sup>193</sup> studies, we can then examine participants' recall sequences by asking which events they tended  
<sup>194</sup> to recall first (probability of first recall; Fig. 3A; Atkinson and Shiffrin, 1968; Postman and Phillips,  
<sup>195</sup> 1965; Welch and Burnett, 1924); how participants most often transition between recalls of the  
<sup>196</sup> events as a function of the temporal distance between them (lag-conditional response probability;  
<sup>197</sup> Fig. 3B; Kahana, 1996); and which events they were likely to remember overall (serial position  
<sup>198</sup> recall analyses; Fig. 3C; Murdock, 1962). Interestingly, for two of these analyses (probability of first  
<sup>199</sup> recall and lag-conditional response probability curves) we observe patterns comparable to classic  
<sup>200</sup> effects from the list-learning literature: namely, a higher probability of initiating recall with the  
<sup>201</sup> first event in the sequence (Fig. 3A) and a higher probability of transitioning to neighboring events  
<sup>202</sup> with an asymmetric forward bias (Fig. 3C). In contrast, we do not observe a pattern comparable to  
<sup>203</sup> the serial position effect (Fig. 3C), but rather we see higher memory for specific events distributed  
<sup>204</sup> somewhat evenly throughout the video.

<sup>205</sup> We can also apply two list-learning-native analyses that describe how participants group items  
<sup>206</sup> in their recall sequences: temporal clustering and semantic clustering (Polyn et al., 2009, see  
<sup>207</sup> *Methods* for details). Temporal clustering refers to the extent to which participants group their  
<sup>208</sup> recall responses according to encoding position. Overall, we found that sequentially viewed video

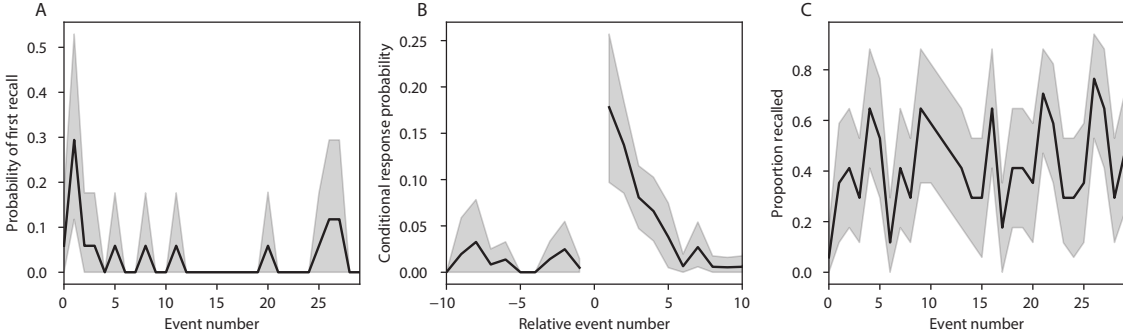


**Figure 3: Naturalistic extensions of classic list-learning memory analyses.** **A.** The probability of first recall as a function of the serial position of the event in the video. **B.** The probability of recalling each event, conditioned on having most recently recalled the event *lag* events away in the video. **C.** The proportion of participants who recalled each event, as a function of the serial position of the events in the video. All panels: error bars denote bootstrap-estimated standard error of the mean.

events were clustered heavily in participants' recall event sequences (mean: 0.767, SEM: 0.029), and that participants with higher temporal clustering scores tended to perform better according to both Chen et al. (2017)'s hand-annotated memory scores (Pearson's  $r(15) = 0.62$ ,  $p = 0.008$ ) and our model's estimate (Pearson's  $r(15) = 0.54$ ,  $p = 0.024$ ). Semantic clustering measures the extent to which participants cluster their recall responses according to semantic similarity. We found that participants tended to recall semantically similar video events together (mean: 0.787, SEM: 0.018), and that semantic clustering score was also related to both hand-annotated (Pearson's  $r(15) = 0.65$ ,  $p = 0.004$ ) and model-derived (Pearson's  $r(15) = 0.63$ ,  $p = 0.007$ ) memory performance.

Statistical models of memory studies often treat recall success as binary (i.e., an item either was or was not recalled), or occasionally categorical (e.g., to distinguish familiarity from recollection; Yonelinas et al., 2002). Such approaches are tenable in classical list-learning or recognition memory paradigms, as the presented stimuli tend to be very simple (e.g., a sequence of individual words or items). However, the feature-rich content of a naturalistic experiences may later be described with many, highly variable levels of success. Our framework produces a content-based model of individual stimulus and recall events by projecting the dynamic content of the video and participants' recalls into a shared topic space. This allows for direct, quantitative comparison

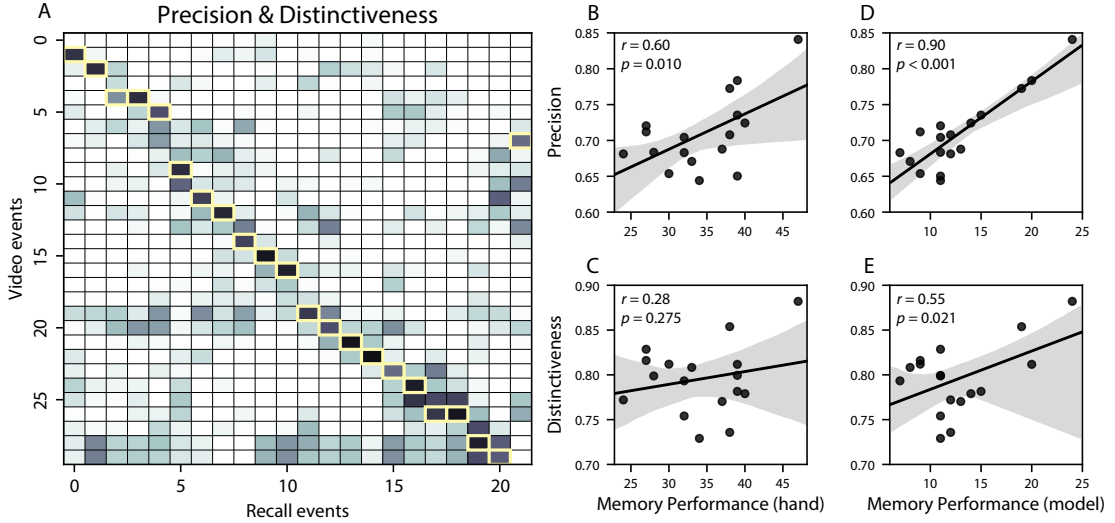


**Figure 4: Novel content-based metrics of naturalistic memory: precision and distinctiveness.** A. The video-recall correlation matrix for a representative participant (17). The yellow boxes highlight the maximum correlation in each column. The example participant's overall precision score was computed as the average across correlation values in the yellow boxes. Their distinctiveness score was computed as the the average (over recall events) of 1 minus the average correlation between each recall event and all other recall events that do not display a box in the same row. B. The (Pearson's) correlation between precision and hand-annotated memory performance. C. The correlation between distinctiveness and hand-annotated memory performance. D. The correlation between precision and the number of video events successfully recalled, as determined by our model. E. The correlation between distinctiveness and the number of video events successfully recalled, as determined by our model.

226 between all stimulus and recall events, as well as between the recall events themselves. Leveraging  
 227 these content-based models of the stimulus/recall events, we developed two novel, *continuous*  
 228 metrics for analyzing naturalistic memory: *precision* and *distinctiveness*. We define precision as  
 229 the “completeness” of recall, or how fully the presented content was recapitulated in memory.  
 230 Under our framework, we quantify this for a given recall event as the correlation between the  
 231 topic proportions of the recall event and the maximally correlated video event (Fig. 4). A second  
 232 novel metric we introduce here is *distinctiveness*, which we define as the “specificity” of recall,  
 233 or how unique the description of a given section of content was, compared to descriptions for  
 234 other sections of content. We quantify this for each recall event as 1 minus the average correlation  
 235 between the given recall event and all other recall events not matched to the same video event.

236 In addition to individual events, one may also use these metrics to describe each participant's  
237 overall performance (i.e., by averaging across a participant's event-wise precision or distinctiveness  
238 scores). Participants whose recall events are more veridical descriptions of what happened in the  
239 video event will presumably have higher precision scores. We find that, across participants,  
240 a higher precision score is correlated to both hand-annotated memory performance (Pearson's  
241  $r(15) = 0.60, p = 0.010$ ) and the number of video events successfully remembered, as determined  
242 by our model (Pearson's  $r(15) = 0.90, p < 0.001$ ). We also hypothesized that participants who  
243 recounted events in a more distinctive way would display better overall memory. We find that  
244 this distinctiveness score is related to our model's estimated number of recalled events (Pearson's  
245  $r(15) = 0.55, p = 0.021$ ), and while we do not find distinctiveness to be related to hand-annotated  
246 memory performance (Pearson's  $r(15) = 0.28, p = 0.275$ ), this is not entirely surprising given how  
247 the hand-annotated memory scores were computed (see *Discussion*).

248 Further intuition for the behaviors captured by these two metrics may be gained by directly  
249 examining the content of the video and recalls our framework models. In Figure 5, we contrast  
250 recalls for the same video event (event 22) from two participants: one with a high precision score  
251 (P17), the other with a low precision score (P6). From the HMM-identified event boundaries,  
252 we recovered the set of annotations describing the content of an example video event (Fig. 5B),  
253 and divided them into different color-coded sections for each action or feature described. We  
254 then similarly recovered the set of sentences comprising the corresponding recall event for each  
255 of the two example participants. Because the recall sliding windows overlap heavily, and each  
256 recall event spans multiple recall timepoints (i.e., windows), we have stripped any sentences from  
257 the beginning and end that describe earlier or later video events for the sake of readability. In  
258 other words, Fig. 5C shows a subset of the full recall event text, comprising sentences between  
259 the first and last descriptions of content from the example video event. We then colored all words  
260 describing actions and features coded in panel B by their corresponding color. Visual comparison  
261 of the transcripts reveals that the most precise participant's recall both captures more of the video  
262 event's content, and does so with far more detail.

263 Figure 6 similarly contrasts two example participants' recalls for a common video event (event

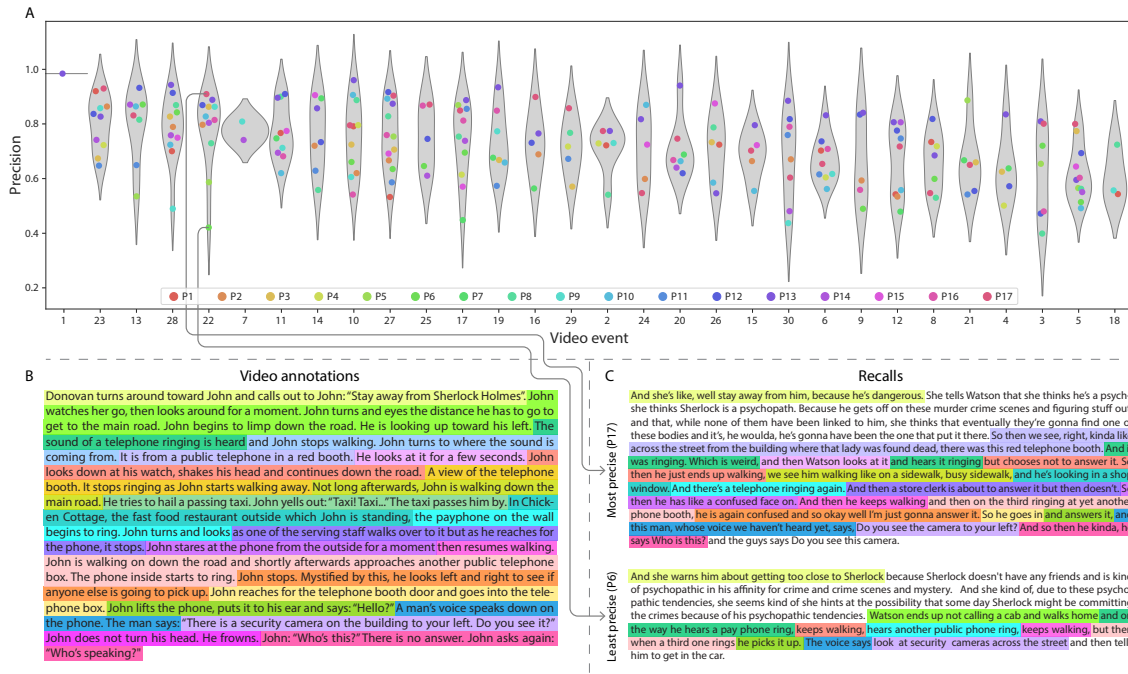


**Figure 5: Precision metric reflects completeness of recall.** **A.** Recall precision by video event. Grey violin plots display kernel density estimates for the distribution of recall precision scores for a single video event. Colored dots within each violin plot represent individual participants' recall precision for the given event. Video events are ordered along the *x*-axis by the average precision with which they were remembered. **B.** The set of "Narrative Details" video annotations (generated by Chen et al., 2017) for scenes comprising an example video event (22) identified by the HMM. Each action or feature is highlighted in a different color. **C.** A subset of the sentences comprising the most precise (P17) and least precise (P6) participants' recalls of video event 22. Descriptions of specific actions or features reflecting those highlighted in panel B are highlighted in the corresponding color.

19) to illustrate the tangible differences between high and low distinctiveness scores. Here, we  
 20) have extracted the full set of sentences comprising the most distinctive recall event (P13) and least  
 21) distinctive recall event (P11) recall event matched to the example video event (Fig. 6C). We also  
 22) extracted the annotations for the example video event, as well as those from each other video  
 23) event whose content the example participants' single recall events described (Fig. 6B). We then  
 24) shaded the annotation text for each video event with a different color, and shaded each word of  
 25) the example participants' recall text by the color of the video event it describes. The majority of  
 26) the most distinctive recall event text describes video event 19's content, with the first five and last  
 27) one sentence describing the video events immediately preceding and succeeding the current one,

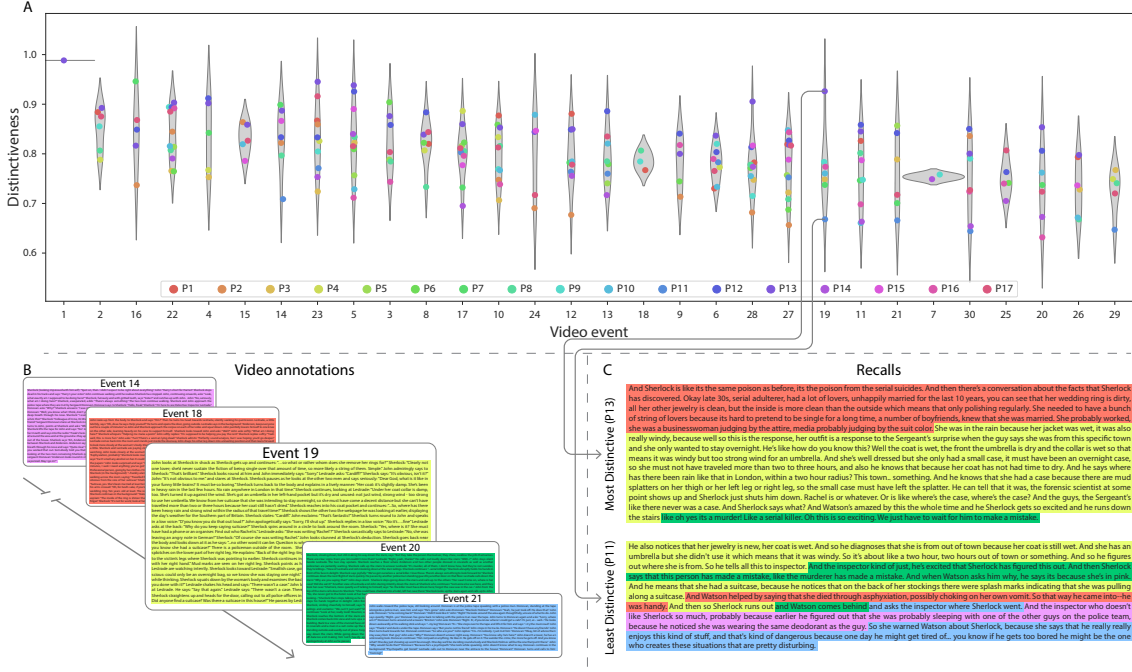


**Figure 6: Distinctiveness metric reflects specificity of recall.** **A.** Recall distinctiveness by video event. Kernel density estimates for each video event’s distribution of recall distinctiveness scores, analogous to Fig. 5A. **B.** The sets of “Narrative Details” video annotations (generated by Chen et al., 2017) for scenes comprising video events described by the example participants in panel C. Each event’s text is highlighted in a different color. **C.** The sentences comprising the most distinctive (P13) and least distinctive (P11) participants’ recalls of video event 19. Sections of recall describing each each video event in panel B are highlighted with the corresponding color.

273 respectively. Meanwhile, the least precise participant’s recall for video event 19 blends the content  
 274 from five separate video events, does not transition between them in order, and often combines  
 275 descriptions of two video events’ content in the same sentence

276 The prior analyses leverage the correspondence between the 100-dimensional topic proportion  
 277 matrices for the video and participants’ recalls to characterize recall. However, it is difficult to  
 278 gain deep insights into the content of (or relationships between) experiences and memories solely  
 279 by examining these topic proportions (e.g., Figs. 2A, D) or the corresponding correlation matrices  
 280 (Figs. 2B, E, S4). And while we can directly examine the original text underlying these topic  
 281 vectors (e.g., Figs. 5, 6) to show how relationships between them reflect real-world behavior, this  
 282 comparison becomes prohibitively cumbersome at larger timescales. To visualize the time-varying

283 high-dimensional content in a more intuitive way (Heusser et al., 2018b) we projected the topic  
284 proportions matrices onto a two-dimensional space using Uniform Manifold Approximation and  
285 Projection (UMAP; McInnes et al., 2018). In this lower-dimensional space, each point represents a  
286 single video or recall event, and the distances between the points reflect the distances between the  
287 events' associated topic vectors (Fig. 7). In other words, events that are nearer to each other in this  
288 space are more semantically similar, and those that are farther apart are less so.

289 Visual inspection of the video and recall topic trajectories reveals a striking pattern. First,  
290 the topic trajectory of the video (which reflects its dynamic content; Fig. 7A) is captured nearly  
291 perfectly by the averaged topic trajectories of participants' recalls (Fig. 7B). To assess the consistency  
292 of these recall trajectories across participants, we asked: given that a participant's recall trajectory  
293 had entered a particular location in topic space, could the position of their *next* recalled event  
294 be predicted reliably? For each location in topic space, we computed the set of line segments  
295 connecting successively recalled events (across all participants) that intersected that location (see  
296 *Methods* for additional details). We then computed (for each location) the distribution of angles  
297 formed by the lines defined by those line segments and a fixed reference line (the *x*-axis). Rayleigh  
298 tests revealed the set of locations in topic space at which these across-participant distributions  
299 exhibited reliable peaks (blue arrows in Fig. 7B reflect significant peaks at  $p < 0.05$ , corrected). We  
300 observed that the locations traversed by nearly the entire video trajectory exhibited such peaks.  
301 In other words, participants exhibited similar trajectories that also matched the trajectory of the  
302 original video (Fig. 7C). This is especially notable when considering the fact that the number of  
303 events participants recalled (dots in Fig. 7C) varied considerably across people, and that every  
304 participant used different words to describe what they had remembered happening in the video.  
305 Differences in the numbers of remembered events appear in participants' trajectories as differences  
306 in the sampling resolution along the trajectory. We note that this framework also provides a  
307 means of disentangling classic "proportion recalled" measures (i.e., the proportion of video events  
308 described in participants' recalls) from participants' abilities to recapitulate the overall unfolding  
309 of the original video's content (i.e., the similarity between the shapes of the original video trajectory  
310 and that defined by each participant's recounting of the video).

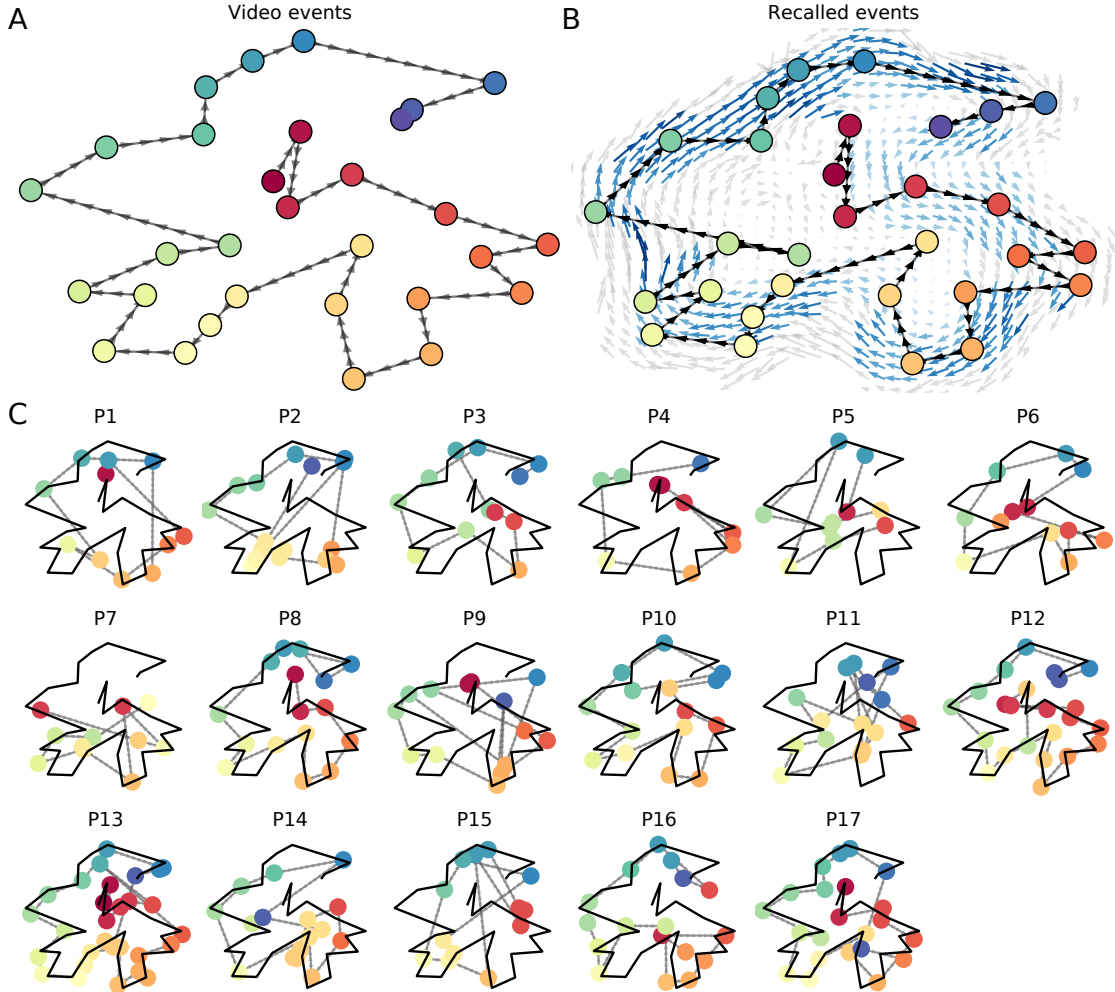


**Figure 7: Trajectories through topic space capture the dynamic content of the video and recalls.** All panels: the topic proportion matrices have been projected onto a shared two-dimensional space using UMAP. **A.** The two-dimensional topic trajectory taken by the episode of *Sherlock*. Each dot indicates an event identified using the HMM (see *Methods*); the dot colors denote the order of the events (early events are in red; later events are in blue), and the connecting lines indicate the transitions between successive events. **B.** The average two-dimensional trajectory captured by participants' recall sequences, with the same format and coloring as the trajectory in Panel A. To compute the event positions, we matched each recalled event with an event from the original video (see *Results*), and then we averaged the positions of all events with the same label. The arrows reflect the average transition direction through topic space taken by any participants whose trajectories crossed that part of topic space; blue denotes reliable agreement across participants via a Rayleigh test ( $p < 0.05$ , corrected). **C.** The recall topic trajectories (gray) taken by each individual participant (P1–P17). The video's trajectory is shown in black for reference. Here, events (dots) are colored by their matched video event (Panel A).

311        The results displayed in Figures 3C and 5A suggest that certain events were remembered better  
312      than others. Given this, we next asked whether the events were generally remembered  
313      well or poorly tended to reflect particular content. Because our analysis framework projects the  
314      dynamic video content and participants' recalls into a shared space, and because the dimensions  
315      of that space represent topics (which are, in turn, sets of weights over words in the vocabulary), we  
316      are able to recover the weighted combination of words that make up any point (i.e., topic vector) in  
317      this space. We first computed the average precision with which participants recalled each of the 30  
318      video events (Fig. 8A; note that this result is analogous to a serial position curve created from our  
319      continuous recall quality metric). We then computed a weighted average of the topic vectors for  
320      each video event, where the weights reflected how reliably each event was recalled. To visualize  
321      the result, we created a "wordle" image (Mueller et al., 2018) where words weighted more heavily  
322      by better-remembered topics appear in a larger font (Fig. 8B, green box). Across the full video,  
323      content that reflected topics necessary to convey the central focus of the video (e.g., the names of the  
324      two main characters, "Sherlock" and "John", and the address of a major recurring location, "221B  
325      Baker Street") were best remembered. An analogous analysis revealed which themes were poorly  
326      remembered. Here in computing the weighted average over events' topic vectors, we weighted  
327      each event in *inverse* proportion to how well it was remembered (Fig. 8B, red box). The least well-  
328      remembered video content reflected information not necessary to later convey a general summary  
329      of the video, such as the proper names of relatively minor characters (e.g., "Mike," "Molly," and  
330      "Lestrade") and locations (e.g., "St. Bartholomew's Hospital").

331        A similar result emerged from assessing the topic vectors for individual video and recall events  
332      (Fig. 8C). Here, for each of the three best- and worst-remembered video events, we have constructed  
333      two wordles: one from the original video event's topic vector (left) and a second from the average  
334      recall topic vector for that event (right). The three best-remembered events (circled in green)  
335      correspond to scenes important to the central plot-line: a mysterious figure spying on John in a  
336      phone booth; John meeting Sherlock at Baker St. to discuss the murders; and Sherlock laying  
337      a trap to catch the killer. Meanwhile, the three worst-remembered events (circled in red) reflect  
338      scenes that are non-essential to summarizing the narrative's structure: the video of singing cartoon

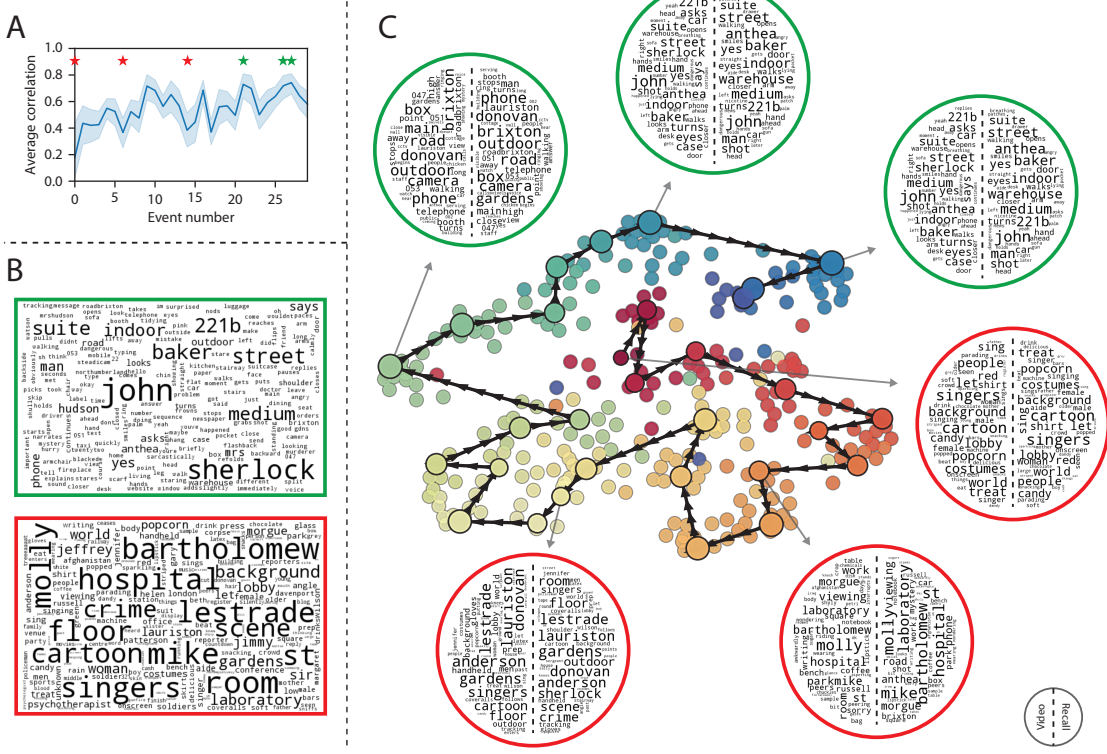


**Figure 8: Transforming experience into memory.** **A.** Average precision (video event-recall event topic vector correlation) across participants for each video event. Error bars denote bootstrap-derived across-participant 95% confidence intervals. The stars denote the three best-remembered events (green) and worst-remembered events (red). **B.** Wordles comprising the top 200 highest-weighted words reflected in the weighted-average topic vector across video events. Green: video events were weighted by how well the topic vectors derived from recalls of those events matched the video events' topic vectors (Panel A). Red: video events were weighted by the inverse of how well their topic vectors matched the recalled topic vectors. **C.** The set of all video and recall events is projected onto the two-dimensional space derived in Figure 7. The dots outlined in black denote video events (dot size reflects the average correlation between the video event's topic vector and the topic vectors from the closest matching recalled events from each participant; bigger dots denote stronger correlations). The dots without black outlines denote recalled events. All dots are colored using the same scheme as Figure 7A. Wordles for several example events are displayed (green: three best-remembered events; red: three worst-remembered events). Within each circular wordle, the left side displays words associated with the topic vector for the video event, and the right side displays words associated with the (average) recall event topic vector, across all recall events matched to the given video event.

339 characters participants viewed prior to the main episode; John asking Molly about Sherlock's habit  
340 of over-analyzing people; and Sherlock noticing evidence of Anderson's and Donovan's affair.

341 The results thus far inform us about which aspects of the dynamic content in the episode partic-  
342 ipants watched were preserved or altered in participants' memories. We next carried out a series  
343 of analyses aimed at understanding which brain structures might facilitate these preservations and  
344 transformations between the external world and memory. In one analysis, we sought to identify  
345 brain structures that were sensitive to the dynamic unfolding of the video's content, as character-  
346 ized by its topic trajectory. We used a searchlight procedure to identify clusters of voxels whose  
347 activity patterns displayed a proximal temporal correlation structure (as participants watched the  
348 video) matching that of the original video's topic proportions (Fig. 9A; see *Methods* for additional  
349 details). In a second analysis, we sought to identify brain structures whose responses (during  
350 video viewing) reflected how each participant would later structure their *recalls* of the video. We  
351 used an analogous searchlight procedure to identify clusters of voxels whose proximal temporal  
352 correlation matrices matched that of the topic proportions for each individual's recall (Figs. 9B; see  
353 *Methods* for additional details). To ensure our searchlight procedure identified regions *specifically*  
354 sensitive to the temporal structure of the video or recalls (i.e., rather than those with a tempo-  
355 ral autocorrelation length similar to that of the video/recalls), we performed a phase shift-based  
356 permutation correction (see *Methods* for additional details). Specifically, we circularly shifted the  
357 timeseries of the topic trajectory by a random number of timepoints, recomputed the shifted tra-  
358 jectory's correlation matrix, and again performed our searchlight analysis on this permuted data.  
359 We then *z*-scored the "real" searchlight results at each voxel against the null distribution of (100)  
360 permuted results. In Figure 9, only voxels whose activity pattern reflected the "real" video/recall  
361 timeseries more closely than 95% of the permuted results are shown. As shown in Figure 9C, the  
362 video-driven searchlight analysis revealed a distributed network of regions that may play a role in  
363 processing information relevant to the narrative structure of the video. Similarly, the recall-driven  
364 searchlight analysis revealed a second diffuse network of regions (Fig. 9D) that may facilitate a  
365 person-specific transformation of one's experience into memory. In identifying regions whose re-  
366 sponses to ongoing experiences reflect how those experiences will be remembered later, this latter

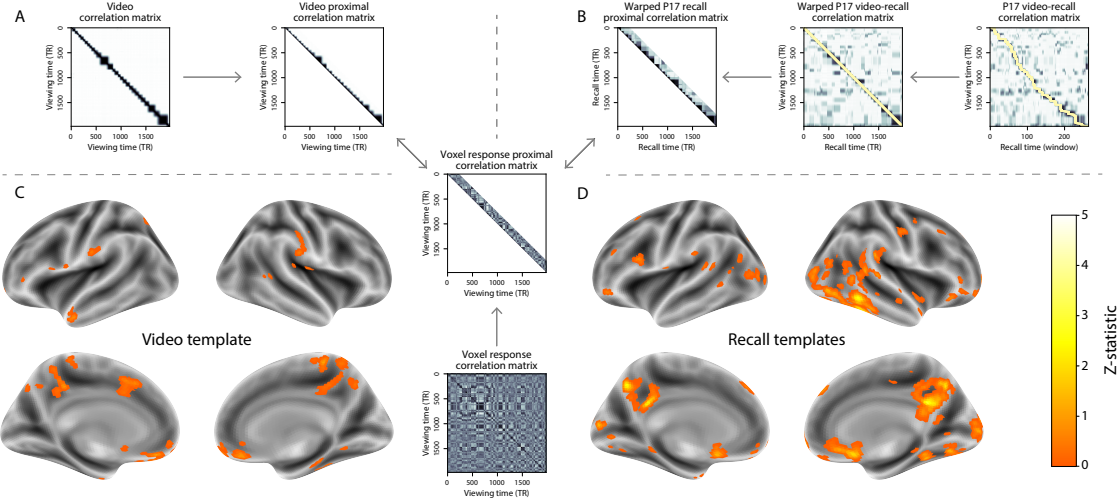


**Figure 9: Brain structures that underlie the transformation of experience into memory.** **A.** We isolated the proximal diagonals from the upper triangle of the video correlation matrix, and applied this same diagonal mask to the voxel response correlation matrix for each cube of voxels in the brain. We then searched for brain regions whose activation timeseries consistently exhibited a similar proximal correlational structure to the video model, across participants. **B.** We used dynamic time warping (Berndt and Clifford, 1994) to align each participant's recall timeseries to the TR timeseries of the video. We then applied the same diagonal mask used in Panel A to isolate the proximal temporal correlations and searched for brain regions whose activation timeseries for an individual consistently exhibited a similar proximal correlational structure to each individual's recall. **C.** We identified a network of regions sensitive to the narrative structure of participants' ongoing experience. The map shown is thresholded at  $p < 0.05$ , corrected. **D.** We also identified a network or regions sensitive to how individuals would later structure the video's content in their recalls. The map shown is thresholded at  $p < 0.05$ , corrected.

367 analysis extends classic *subsequent memory analyses* (e.g., Paller and Wagner, 2002) to domain of  
 368 naturalistic stimuli.

369 The searchlight analyses described above yielded two distributed networks of brain regions,  
 370 whose activity timecourses mirrored to the temporal structure of the video (Fig. 9C) or partici-  
 371 pants' eventual recalls (Fig. 9D). We next sought to gain greater insight into the structures and  
 372 functional networks our results reflected. To accomplish this in a blind, unbiased manner (i.e.,  
 373 without reverse inference via visual observation) we performed an additional, exploratory analy-  
 374 sis using Neurosynth (Yarkoni et al., 2011). Neurosynth parses a massive online database of over  
 375 14,000 neuroimaging studies and constructs meta-analysis images for over 13,000 psychology-  
 376 and neuroscience-related terms, based on NIFTI images accompanying studies where those terms

<sup>377</sup> appear at a high frequency. Then, given a novel image (tagged with its value type; e.g.,  $t$ -,  $F$ - or  
<sup>378</sup>  $p$ -statistics), Neurosynth returns a list of terms whose meta-analysis images are most similar to this  
<sup>379</sup> new data. Our permutation procedure (described above) yielded, for each of the two searchlight  
<sup>380</sup> analyses, a voxelwise map of significance ( $p$ -statistic) values. These maps describe the extent to  
<sup>381</sup> which each voxel *specifically* reflected the temporal structure of the video or individuals' recalls (i.e.,  
<sup>382</sup> for each voxel, the proportion of phase-shifted topic vector correlation matrices less similar to the  
<sup>383</sup> voxel activity correlation matrix than the unshifted video's correlation matrix). These significance  
<sup>384</sup> maps for the video- and recall-driven searchlight analyses, along with the 10 terms with maximally  
<sup>385</sup> similar meta-analysis images identified by Neurosynth are shown in Figure 10.

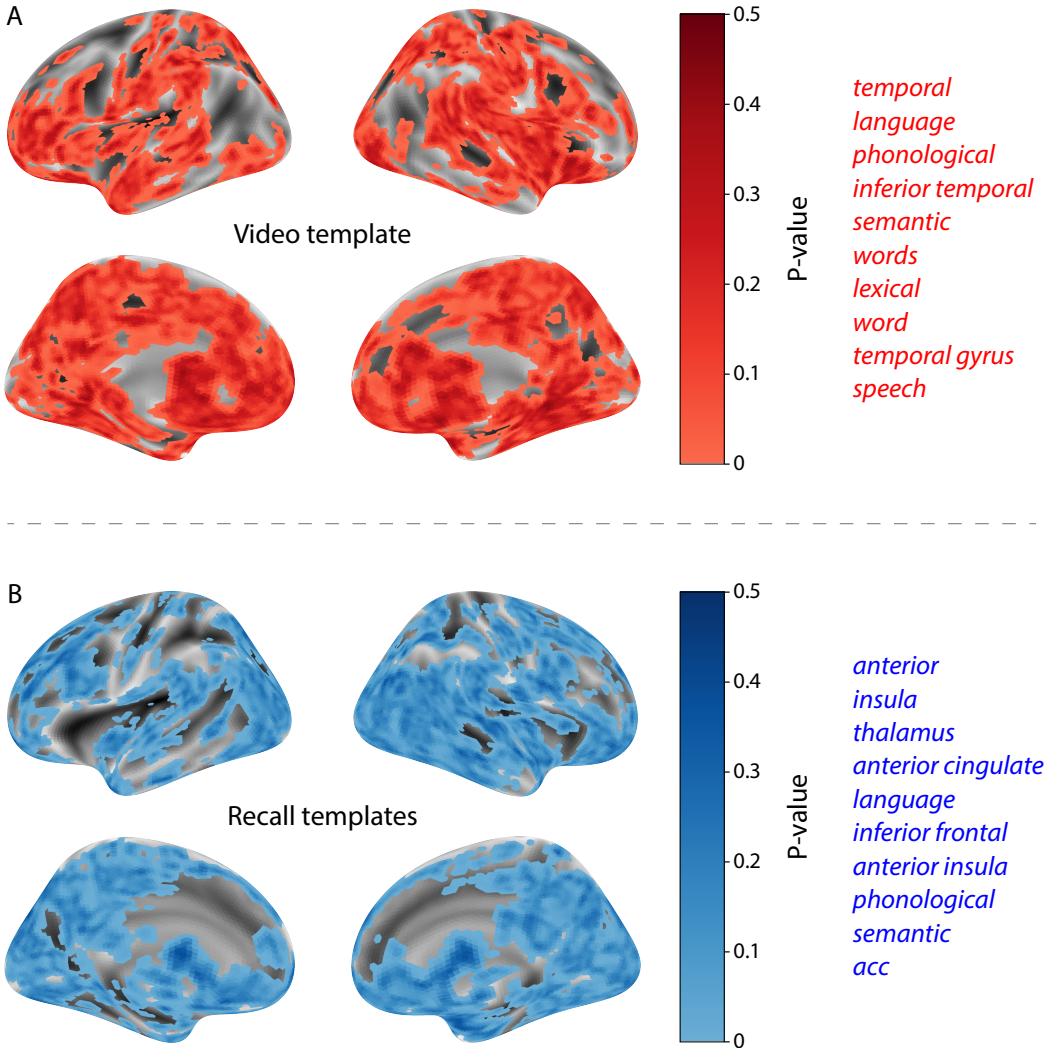


**Figure 10: Decoding distributed statistical maps via Neurosynth meta-analyses.** **A.** Video-searchlight significance and top 10 decoded terms. We constructed a map of the permutation-derived  $p$ -values for the video-driven searchlight analysis (Fig. 9A, C) at each voxel with a positive permutation-derived  $z$ -score. The top 10 terms decoded from this significance map are shown in red. **B.** Recall-searchlight significance and top 10 decoded terms. We constructed a map of the permutation-derived  $p$ -values for the recall-driven searchlight analysis (Fig. 9A, C) at each voxel with a positive permutation-derived  $z$ -score. The top 10 terms decoded from this significance map are shown in blue.

386 **Discussion**

387 Our work casts remembering as reproducing (behaviorally and neurally) the topic trajectory, or  
388 shape, of an experience. This view draws inspiration from prior work aimed at elucidating  
389 the neural and behavioral underpinnings of how we process dynamic naturalistic experiences  
390 and remember them later. One approach to identifying neural responses to naturalistic stimuli  
391 (including experiences) entails building a model of the stimulus and searching for brain regions  
392 whose responses are consistent with the model. In prior work, a series of studies from Uri Hasson's  
393 group (Lerner et al., 2011; Simony et al., 2016; Chen et al., 2017; Baldassano et al., 2017; Zadbood  
394 et al., 2017) have extended this approach with a clever twist: rather than building an explicit  
395 stimulus model, these studies instead search for brain responses (while experiencing the stimulus)  
396 that are reliably similar across individuals. So called *inter-subject correlation* (ISC) and *inter-subject*  
397 *functional connectivity* (ISFC) analyses effectively treat other people's brain responses to the stimulus  
398 as a "model" of how its features change over time. By contrast, in our present work, we use topic  
399 models to construct an explicit content model directly from the stimulus (i.e., the topic trajectory  
400 of the video). Projecting each participant's recall into a space shared by both the stimulus and  
401 other participants then allows us to compare recalls both directly to the stimulus and to each other.  
402 Similarly, prior work introducing the use of HMMs to discover latent event structure in naturalistic  
403 stimuli and recall (Baldassano et al., 2017) used between-subjects cross-validation to identify event  
404 boundaries shared across participants, and between stimulus and recall. Our framework allows  
405 us to break from the restriction of a common, shared event-timeseries and identify the unique  
406 *resolution* of each participant's recall event structure, and how that may differ from the video and  
407 that of other participants.

408 While a large number of language models exist (e.g., WAS, LSA, word2vec, universal sentence  
409 encoder; Steyvers et al., 2004; Landauer et al., 1998; Mikolov et al., 2013; Cer et al., 2018), here  
410 we use latent dirichlet allocation (LDA)-based topic models for a few reasons. First, topic models  
411 capture the *essence* of a text passage devoid of the specific set and order of words used. This was  
412 an important feature of our model since different people may accurately recall a scene using very

413 different language. Second, words can mean different things in different contexts (e.g. “bat” may  
414 be the act of hitting a baseball, the object used for that action, or as a flying mammal). Topic  
415 models are robust to this, allowing words to exist as part of multiple topics. Last, topic models  
416 provide a straightforward means to recover the weights for the particular words comprising a topic,  
417 enabling easy interpretation of an event’s contents (e.g. Fig. 8). Other models such as Google’s  
418 Universal Sentence Encoder offer a context-sensitive encoding of text passages, but the encoding  
419 space is complex and non-linear, and thus recovering the original words used to fit the model is  
420 not straightforward. However, it’s worth pointing out that our framework is divorced from the  
421 particular choice of language model. Moreover, many of the aspects of our framework could be  
422 swapped out for other choices. For example, the language model, the timeseries segmentation  
423 model and the video-recall matching function could all be customized for the particular problem.  
424 Indeed for some problems, recovery of the particular recall words may not be necessary, and thus  
425 other text-modeling approaches (such as universal sentence encoder) may be preferable. Future  
426 work will explore the influence of particular model choices on the framework’s efficacy.

427 In extending classical free recall analyses to our naturalistic memory framework, we recovered  
428 two patterns of recall dynamics central to list-learning studies: a heightened probability of initiating  
429 recall with the first presented “item” (in our case, video events; Fig. 3A) and a strong bias toward  
430 transitioning from recalling a given event to recalling the one immediately following it (Fig. 3B).  
431 However, equally noteworthy are the typical free recall results *not* recovered in these analyses,  
432 as each highlights a fundamental difference between the list-learning paradigm and naturalistic  
433 memory paradigms like the one employed in the present study. The most noticeable departure  
434 from hallmark free recall dynamics in these findings is the apparent lack of a serial position effect in  
435 Figure 3C, which instead shows greater and lesser recall probabilities for events distributed across  
436 the video. Stimuli in free recall experiments most often comprise lists of simple, common words,  
437 presented to participants in a random order. (In fact, numerous word pools have been developed  
438 based on these criteria; e.g., Friendly et al., 1982). These stimulus qualities enable two assumptions  
439 that are central to word list analyses, but frequently do not hold for real-world experiences. First,  
440 researchers conducting list-learning experiments may assume that the content at each presentation

441 index is essentially equal, and does not possess attributes that would render it, on average, more  
442 or less memorable than others. Such is rarely the case with real-world experiences or experiments  
443 meant to approximate them, and the effects of both intrinsic and observer-dependent factors on  
444 stimulus memorability are well established (for review see Chun and Turk-Browne, 2007; Bylinskii  
445 et al., 2015; Tyng et al., 2017). Second, the random ordering of list items ensures that (across  
446 participants, on average) there is no relationship between the thematic similarity of individual  
447 stimuli and their presentation positions—in other words, two successively presented items are no  
448 more likely to be highly semantically similar than they are to be high dissimilar. In most cases, the  
449 exact opposite is true of real-world episodes. Our internal thoughts, our actions, and the physical  
450 state of the world around us all tend to follow a direct, causal progression. As a result, each moment  
451 of our experience tends to be inherently more similar to surrounding moments than to those in  
452 the distant past or future. Memory literature has termed this strong temporal autocorrelation  
453 “context,” and in various media that depict real-world events (e.g., movies or written stories),  
454 we recognize it as a *narrative structure*. While a random word list (by definition) has no such  
455 structure, the logical progression between ideas and actions in a naturalistic stimulus prompts the  
456 rememberer to recount presented events in order, starting with the beginning. This tendency is  
457 reflected in our findings’ second departure from typical free recall dynamics: a lack of increased  
458 probability of first recall for end-of-sequence events (Fig. 3A).

459 Because they disregard presentation order-dependent variability in the stimulus content, anal-  
460 yses such as those in Figure 3 enable a more sensitive analysis of presentation order-dependent  
461 temporal dynamics in free recall. Yet by the same token, they paint a wholly incomplete picture of  
462 memory for naturalistic episodes. In an attempt to address this shortcoming, we have developed a  
463 framework in the present study that characterizes the explicit semantic content of the stimulus and  
464 subsequent recalls. However, sensitivity to stimulus and recall content introduces a new challenge:  
465 distinguishing between levels of recall quality for a stimulus (e.g., an event) that is considered to  
466 have been “remembered.” When modeling memory in an experimental setting, recall quality for  
467 individual events is often cast as binary (e.g., a given list item was simply either remembered or  
468 not remembered). Various models of memory (e.g., Yonelinas, 2002) attempt to improve upon this

469 by including confidence ratings, rendering this binary judgement instead categorical. To better  
470 evaluate naturalistic memory quality, we introduce a continuous metric (*precision*), which reflects  
471 the level of completeness of a participant’s recall for a feature-rich experience. Additionally, recall  
472 quality for a single event is typically assessed independently from that for all other events (e.g., it  
473 is difficult to “compare” a participant’s binary recall success for list item 1 to that of list item 10).  
474 The second novel metric we introduce (*distinctiveness*) is based on analyzing of the correlational  
475 structure of an individual’s full set of recall events, and reflects the specificity of their memory  
476 for a single experienced event. We find that both of these metrics relate to the overall number of  
477 video events participants successfully recalled, and that our precision metric additionally relates to  
478 Chen et al. (2017)’s hand-annotated memory memory scores. Though we do not find participants’  
479 average recall distinctiveness related to the hand-annotated memory scores, this is not entirely  
480 surprising given the divergence of behavior they capture. In hand-scoring each participant’s ver-  
481 bal recall for each of 50 (manually-delimited) scenes, “[a] scene was counted as recalled if the  
482 participant described any part of the scene” (Chen et al., 2017). In other words, both an extensive  
483 description of a scene’s content and a brief mention of some subset of its content were (binarily)  
484 considered equally successful recalls. By contrast, we identify the event structure in participants’  
485 recalls in an unsupervised manner, independent of the video event-timeseries, prior to mapping  
486 between video and recall content. Our HMM-based event-segmentation produces boundaries  
487 between timepoints where the topic proportions shift in a substantial way, and because a small  
488 handful of words is unlikely to contribute significantly to the topic proportions for any sliding win-  
489 dow, such brief scene descriptions will most often not begat a sufficiently large shift in the resulting  
490 topic proportions for the HMM to identify an event boundary. Instead, they will be grouped with  
491 a neighboring event, consequently lowering that event’s distinctiveness score and by extension,  
492 the participant’s overall distinctiveness score. This is in essence the qualitative difference between  
493 distinctive and indistinctive recall, and reflects the comparison shown in Figure 6C. Intriguingly,  
494 prior studies show that pattern separation, or the ability to cleanly discriminate between similar  
495 experiences, is impaired in many cognitive disorders as well as natural aging (Stark et al., 2010;  
496 Yassa et al., 2011; Yassa and Stark, 2011). Future work might explore whether and how these

497 metrics compare between cognitively impoverished groups and healthy controls.

498 In the analyses outlined in Figure 9, we identified two diffuse networks of brain structures whose  
499 responses were consistent with the video and recall topic trajectories, respectively. Decoding the  
500 associated significance maps with Neurosynth revealed two intriguing results. First, the top 10  
501 terms returned for the video-driven searchlight significance map were centered around themes of  
502 language and semantic meaning (Fig. 10A). In other words, the voxels identified as more reflective  
503 of the video's temporal structure (i.e., voxels with lower permutation correction-derived  $p$ -values),  
504 as defined by our model, were most likely to be reported as active in studies focused on the neural  
505 underpinnings of semantic processing. This finding is interesting, as our model specifically  
506 captures the temporal structure of the video's *semantic* content (e.g., as opposed to that of the  
507 visual, auditory, or affective content). This suggests that the network of structures displayed in  
508 Figure 9C may play a role in processing the evolving semantic structure of ongoing experiences.

509 Our second searchlight analysis identified a largely separate network of regions (Fig. 9D)  
510 whose patterns of activity as participants viewed the video reflected the idiosyncratic structure  
511 of each individual's later recall. Decoding the associated significance map yielded a set of terms  
512 that primarily reflected names of specific structural regions (such as "thalamus," "anterior insula,"  
513 "anterior cingulate" and "inferior frontal"; Fig. 10B). Interestingly, these regions share membership  
514 in a common, large-scale functional network (termed the "salience network") involved in detecting  
515 and processing affective cues. In particular, the latter three regions have been implicated in  
516 functions relevant to assigning personal meaning to an experience, including: ascribing subjective  
517 value to raw, sensory input (Medford and Critchley, 2010); modulating semantic and phonological  
518 processing in response to personally salient stimuli (Kelly et al., 2007); and directing and reallocating  
519 attention and working memory resources towards the most relevant stimuli (Menon and  
520 Uddin, 2010). This suggests that the network of structures displayed in Figure 9D may play a  
521 role in transforming and restructuring ongoing experiences through the lens of one's own personal  
522 values as they are encoded in memory.

523 Our work has broad implications for how we characterize and assess memory in real-world  
524 settings, such as the classroom or physician's office. For example, the most commonly used

525 classroom evaluation tools involve simply computing the proportion of correctly answered exam  
526 questions. Our work indicates that this approach is only loosely related to what educators might  
527 really want to measure: how well did the students understand the key ideas presented in the  
528 course? Under this typical framework of assessment, the same exam score of 50% could be  
529 ascribed to two very different students: one who attended the full course but struggled to learn  
530 more than a broad overview of the material, and one who attended only half of the course but  
531 understood the material perfectly. Instead, one could apply our computational framework to build  
532 explicit content models of the course material and exam questions. This approach would provide  
533 a more nuanced and specific view into which aspects of the material students had learned well  
534 (or poorly). In clinical settings, memory measures that incorporate such explicit content models  
535 might also provide more direct evaluations of patients' memories.

## 536 Methods

### 537 Experimental design and data collection

538 Data were collected by Chen et al. (2017). In brief, participants ( $n = 22$ ) viewed the first 48 minutes  
539 of "A Study in Pink", the first episode of the BBC television series *Sherlock*, while fMRI volumes  
540 were collected (TR = 1500 ms). Participants were pre-screened to ensure they had never seen any  
541 episode of the show before. The stimulus was divided into a 23 min (946 TR) and a 25 min (1030 TR)  
542 segment to mitigate technical issues related to the scanner. After finishing the clip, participants  
543 were instructed to (quoting from Chen et al., 2017) "describe what they recalled of the [episode]  
544 in as much detail as they could, to try to recount events in the original order they were viewed  
545 in, and to speak for at least 10 minutes if possible but that longer was better. They were told that  
546 completeness and detail were more important than temporal order, and that if at any point they  
547 realized they had missed something, to return to it. Participants were then allowed to speak for  
548 as long as they wished, and verbally indicated when they were finished (e.g., 'I'm done')." Five  
549 participants were dropped from the original dataset due to excessive head motion (2 participants),

550 insufficient recall length (2 participants), or falling asleep during stimulus viewing (1 participant),  
551 resulting in a final sample size of  $n = 17$ . For additional details about the experimental procedure  
552 and scanning parameters, see Chen et al. (2017). The experimental protocol was approved by  
553 Princeton University's Institutional Review Board.

554 After preprocessing the fMRI data and warping the images into a standard ( $3 \text{ mm}^3$  MNI) space,  
555 the voxel activations were z-scored (within voxel) and spatially smoothed using a 6 mm (full width  
556 at half maximum) Gaussian kernel. The fMRI data were also cropped so that all video-viewing  
557 data were aligned across participants. This included a constant 3 TR (4.5 s) shift to account for the  
558 lag in the hemodynamic response. (All of these preprocessing steps followed Chen et al., 2017,  
559 where additional details may be found.)

560 The video stimulus was divided into 1,000 fine-grained “scenes” and annotated by an inde-  
561 pendent coder. For each of these 1,000 scenes, the following information was recorded: a brief  
562 narrative description of what was happening, the location where the scene took place, whether  
563 that location was indoors or outdoors, the names of all characters on-screen, the name(s) of the  
564 character(s) in focus in the shot, the name(s) of the character(s) currently speaking, the camera  
565 angle of the shot, a transcription of any text appearing on-screen, and whether or not there was  
566 music present in the background. Each scene was also tagged with its onset and offset time, in  
567 both seconds and TRs.

## 568 **Data and code availability**

569 The fMRI data we analyzed are available online [here](#). The behavioral data and all of our analysis  
570 code may be downloaded [here](#).

## 571 **Statistics**

572 All statistical tests performed in the behavioral analyses were two-sided. All statistical tests per-  
573 formed in the neural data analyses were two-sided, except for the permutation-based thresholding,  
574 which was one-sided. In this case, we were specifically interested in identifying voxels whose ac-

575 tivation time series reflected the temporal structure of the video and recall trajectories to a *greater*  
576 extent than that of the phase-shifted trajectories.

577 **Modeling the dynamic content of the video and recall transcripts**

578 **Topic modeling**

579 The input to the topic model we trained to characterize the dynamic content of the video comprised  
580 998 hand-generated annotations of short (mean: 2.96s) scenes spanning the video clip (Chen et al.,  
581 2017 generated 1000 annotations total; we removed two referring to the break between the first  
582 and second scan sessions, during which no fMRI data was collected). We concatenated the text  
583 for all of the annotated features within each segment, creating a “bag of words” describing each  
584 scene and performed some minor preprocessing (e.g., stemming possessive nouns and removing  
585 punctuation). We then re-organized the text descriptions into overlapping sliding windows span-  
586 ning (up to) 50 scenes each. In other words, we created a “context” for each scene comprising the  
587 text descriptions of the preceding 25 scenes, the present scene, and the following 24 scenes. To  
588 model the “context” for scenes near the beginning and end of the video (i.e., within 25 scenes of  
589 the beginning or end), we created overlapping sliding windows that grew in size from one scene  
590 to the full length, then similarly tapered their length at the end. This additionally ensured that  
591 each scene’s content was represented in the text corpus an equal number of times.

592 We trained our model using these overlapping text samples with `scikit-learn` (version 0.19.1;  
593 Pedregosa et al., 2011), called from our high-dimensional visualization and text analysis software,  
594 `HyperTools` (Heusser et al., 2018b). Specifically, we used the `CountVectorizer` class to transform  
595 the text from each window into a vector of word counts (using the union of all words across all  
596 scenes as the “vocabulary,” excluding English stop words); this yielded a number-of-windows  
597 by number-of-words *word count* matrix. We then used the `LatentDirichletAllocation` class  
598 (`topics=100, method='batch'`) to fit a topic model (Blei et al., 2003) to the word count matrix,  
599 yielding a number-of-windows (1047) by number-of-topics (100) *topic proportions* matrix. The  
600 topic proportions matrix describes the gradually evolving mix of topics (latent themes) present in

601 each scene. Next, we transformed the topic proportions matrix to match the 1976 fMRI volume  
602 acquisition times. We assigned each topic vector to the timepoint (in seconds) midway between the  
603 beginning of the first scene and the end of the last scene in its corresponding sliding text window.  
604 By doing so, we warped the linear temporal distance between consecutive topic vectors to align  
605 with the inconsistent temporal distance between consecutive annotations (whose durations varied  
606 greatly). We then rescaled these timepoints to 1.5s TR units, and used linear interpolation to  
607 estimate a topic vector for each TR. This resulted in a number-of-TRs (1976) by number-of-topics  
608 (100) matrix.

609 We created similar topic proportions matrices using hand-annotated transcripts of each par-  
610 ticipant’s recall of the video (annotated by Chen et al., 2017). We tokenized the transcript into a  
611 list of sentences, and then re-organized the list into overlapping sliding windows spanning (up  
612 to) 10 sentences each, analogously to how we parsed the video annotations. In turn, we trans-  
613 formed each window’s sentences into a word count vector (using the same vocabulary as for the  
614 video model), then used the topic model already trained on the video scenes to compute the most  
615 probable topic proportions for each sliding window. This yielded a number-of-windows (range:  
616 83–312) by number-of-topics (100) topic proportions matrix for each participant. These reflected  
617 the dynamic content of each participant’s recalls. Note: for details on how we selected the video  
618 and recall window lengths and number of topics, see *Supporting Information* and Figure S1.

### 619 **Parsing topic trajectories into events using Hidden Markov Models**

620 We parsed the topic trajectories of the video and participants’ recalls into events using Hidden  
621 Markov Models (Rabiner, 1989). Given the topic proportions matrix (describing the mix of topics  
622 at each timepoint) and a number of states,  $K$ , an HMM recovers the set of state transitions that  
623 segments the timeseries into  $K$  discrete states. Following Baldassano et al. (2017), we imposed an  
624 additional set of constraints on the discovered state transitions that ensured that each state was  
625 encountered exactly once (i.e., never repeated). We used the BrainIAK toolbox (Capota et al., 2017)  
626 to implement this segmentation.

627 We used an optimization procedure to select the appropriate  $K$  for each topic proportions

628 matrix. Prior studies on narrative structure and processing have shown that we both perceive  
629 and internally represent the world around us at multiple, hierarchical timescales (e.g., Hasson  
630 et al., 2008; Lerner et al., 2011; Hasson et al., 2015; Chen et al., 2017; Baldassano et al., 2017, 2018).  
631 However, for the purposes of our framework, we sought to identify the single timeseries of event-  
632 representations that is emphasized *most heavily* in the temporal structure of the video and of each  
633 participant's recall. We quantified this as the set of  $K$  states that maximized the similarity between  
634 topic vectors for timepoints comprising each state, while minimizing the similarity between topic  
635 vectors for timepoints across different states. Specifically, we computed (for each matrix)

$$\operatorname{argmax}_K [W_1(a, b)],$$

636 where  $a$  was the distribution of within-state topic vector correlations, and  $b$  was the distribution of  
637 across-state topic vector correlations . We computed the first Wasserstein distance ( $W_1$ ; also known  
638 as "earth mover's distance"; Dobrushin, 1970; Ramdas et al., 2017) between these distributions for a  
639 large range of possible  $K$ -values (range [2,50]), and selected the  $K$  that yielded the maximum value.  
640 Figure 2B displays the event boundaries returned for the video, and Figure S4 displays the event  
641 boundaries returned for each participant's recalls. See Figure S6 for the optimization functions  
642 for the video and recalls. After obtaining these event boundaries, we created stable estimates of  
643 the content represented in each event by averaging the topic vectors across timepoints between  
644 each pair of event boundaries. This yielded a number-of-events by number-of-topics matrix for  
645 the video and recalls from each participant.

#### 646 **Naturalistic extensions of classic list-learning analyses**

647 In traditional list-learning experiments, participants view a list of items (e.g., words) and then recall  
648 the items later. Our video-recall event matching approach affords us the ability to analyze memory  
649 in a similar way. The video and recall events can be treated analogously to studied and recalled  
650 "items" in a list-learning study. We can then extend classic analyses of memory performance and  
651 dynamics (originally designed for list-learning experiments) to the more naturalistic video recall

652 task used in this study.

653 Perhaps the simplest and most widely used measure of memory performance is *accuracy*—i.e.,  
654 the proportion of studied (experienced) items (in this case, video events) that the participant later  
655 remembered. Chen et al. (2017) used this method to rate each participant’s memory quality by  
656 computing the proportion of (50, manually identified) scenes mentioned in their recall. We found a  
657 strong across-participants correlation between these independent ratings and the proportion of (30,  
658 HMM-identified) video events matched to participants’ recalls (Pearson’s  $r(15) = 0.71, p = 0.002$ ).  
659 We further considered a number of more nuanced memory performance measures that are typically  
660 associated with list-learning studies. We also provide a software package, Quail, for carrying out  
661 these analyses (Heusser et al., 2017).

662 **Probability of first recall (PFR).** PFR curves (Welch and Burnett, 1924; Postman and Phillips,  
663 1965; Atkinson and Shiffrin, 1968) reflect the probability that an item will be recalled first as a  
664 function of its serial position during encoding. To carry out this analysis, we initialized a number-  
665 of-participants (17) by number-of-video-events (30) matrix of zeros. Then for each participant, we  
666 found the index of the video event that was recalled first (i.e., the video event whose topic vector  
667 was most strongly correlated with that of the first recall event) and filled in that index in the matrix  
668 with a 1. Finally, we averaged over the rows of the matrix, resulting in a 1 by 30 array representing  
669 the proportion of participants that recalled an event first, as a function of the order of the event’s  
670 appearance in the video (Fig. 3A).

671 **Lag conditional probability curve (lag-CRP).** The lag-CRP curve (Kahana, 1996) reflects the  
672 probability of recalling a given item after the just-recalled item, as a function of their relative  
673 encoding positions (or *lag*). In other words, a lag of 1 indicates that a recalled item was presented  
674 immediately after the previously recalled item, and a lag of -3 indicates that a recalled item came  
675 3 items before the previously recalled item. For each recall transition (following the first recall),  
676 we computed the lag between the current recall event and the next recall event, normalizing by  
677 the total number of possible transitions. This yielded a number-of-participants (17) by number-

678 of-lags (-29 to +29; 61 lags total) matrix. We averaged over the rows of this matrix to obtain a  
679 group-averaged lag-CRP curve (Fig. 3B).

680 **Serial position curve (SPC).** SPCs (Murdock, 1962) reflect the proportion of participants that  
681 remember each item as a function of the items' serial positions during encoding. We initialized  
682 a number-of-participants (17) by number-of-video-events (30) matrix of zeros. Then, for each  
683 recalled event, for each participant, we found the index of the video event that the recalled event  
684 most closely matched (via the correlation between the events' topic vectors) and entered a 1 into  
685 that position in the matrix. This resulted in a matrix whose entries indicated whether or not each  
686 event was recalled by each participant (depending on whether the corresponding entires were  
687 set to one or zero). Finally, we averaged over the rows of the matrix to yield a 1 by 30 array  
688 representing the proportion of participants that recalled each event as a function of the events'  
689 order appearance in the video (Fig. 3C).

690 **Temporal clustering scores.** Temporal clustering describes a participant's tendency to organize  
691 their recall sequences by the learned items' encoding positions. For instance, if a participant  
692 recalled the video events in the exact order they occurred (or in exact reverse order), this would  
693 yield a score of 1. If a participant recalled the events in random order, this would yield an expected  
694 score of 0.5. For each recall event transition (and separately for each participant), we sorted  
695 all not-yet-recalled events according to their absolute lag (i.e., distance away in the video). We  
696 then computed the percentile rank of the next event the participant recalled. We averaged these  
697 percentile ranks across all of the participant's recalls to obtain a single temporal clustering score  
698 for the participant.

699 **Semantic clustering scores.** Semantic clustering describes a participant's tendency to recall se-  
700 mantically similar presented items together in their recall sequences. Here, we used the topic  
701 vectors for each event as a proxy for its semantic content. Thus, the similarity between the seman-  
702 tic content for two events can be computed by correlating their respective topic vectors. For each  
703 recall event transition, we sorted all not-yet-recalled events according to how correlated the topic

704 vector of the closest-matching video event was to the topic vector of the closest-matching video event  
705 to the just-recalled event. We then computed the percentile rank of the observed next recall. We  
706 averaged these percentile ranks across all of the participant's recalls to obtain a single semantic  
707 clustering score for the participant.

708 **Novel naturalistic memory metrics**

709 **Precision.** We tested whether participants who recalled more events were also more *precise* in  
710 their recollections. For each participant, we computed the average correlation between the topic  
711 vectors for each recall event and those of its closest-matching video event. This gave a single value  
712 per participant representing the average precision across all recalled events. We then correlated  
713 these values with both hand-annotated and model-derived (i.e., the number of unique video events  
714 matched by a participant's recall events) memory performance.

715 **Distinctiveness.** We also considered the *distinctiveness* of each recalled event. That is, how unique  
716 a participant's description of a video event was, versus their descriptions of other video events.  
717 We hypothesized that participants with high memory performance might describe each event in  
718 a more distinctive way (relative to those with lower memory performance who might describe  
719 events in a more general way). To test this hypothesis we define a distinctiveness score for each  
720 recall event as

$$d(\text{event}) = 1 - \bar{c}(\mathbb{P} \setminus \{\text{event}\}),$$

721 where  $\bar{c}(\mathbb{P} \setminus \{\text{event}\})$  is the average correlation between the given recall event's topic vector and  
722 the topic vectors from all other recall events not matched to the same video event (for a single  
723 participant). We then averaged these distinctiveness scores across all of the events recalled by the  
724 given participant and correlated resulting values with hand-annotated and model derived memory  
725 performance scores across-subjects, as above.

726 Note: in all instances where we performed statistical tests involving precision or distinctiveness

727 scores, we used Fisher’s  $z$ -transformation (Fisher, 1925) to stabilize the variance across the dis-  
728 tribution of correlation values prior to performing the test. Similarly, when averaging precision  
729 or distinctiveness scores, we  $z$ -transformed the scores prior to computing the mean, and inverse  
730  $z$ -transformed the result.

731 **Visualizing the video and recall topic trajectories**

732 We used the UMAP algorithm (McInnes et al., 2018) to project the 100-dimensional topic space  
733 onto a two-dimensional space for visualization (Figs. 7, 8). Importantly, to ensure that all of  
734 the trajectories were projected onto the *same* lower dimensional space, we computed the low-  
735 dimensional embedding on a “stacked” matrix created by vertically concatenating the events-  
736 by-topics topic proportions matrices for the video, across-participants average recall and all 17  
737 individual participants’ recalls. We then divided the rows of the result (a total-number-of-events  
738 by two matrix) back into separate matrices for the video topic trajectory and the trajectories for  
739 each participant’s recalls (Fig. 7). This general approach for discovering a shared low-dimensional  
740 embedding for a collections of high-dimensional observations follows Heusser et al. (2018b). Note:  
741 for further details on how we created this low-dimensional embedding space, see *Supporting  
742 Information*.

743 **Estimating the consistency of flow through topic space across participants**

744 In Figure 7B, we present an analysis aimed at characterizing locations in topic space that dif-  
745 ferent participants move through in a consistent way (via their recall topic trajectories). The  
746 two-dimensional topic space used in our visualizations (Fig. 7) comprised a  $60 \times 60$  (arbitrary  
747 units) square. We tiled this space with a  $50 \times 50$  grid of evenly spaced vertices, and defined a  
748 circular area centered on each vertex whose radius was two times the distance between adjacent  
749 vertices (i.e., 2.4 units). For each vertex, we examined the set of line segments formed by connecting  
750 each pair successively recalled events, across all participants, that passed through this circle. We  
751 computed the distribution of angles formed by those segments and the  $x$ -axis, and used a Rayleigh  
752 test to determine whether the distribution of angles was reliably “peaked” (i.e., consistent across

753 all transitions that passed through that local portion of topic space). To create Figure 7B we drew  
754 an arrow originating from each grid vertex, pointing in the direction of the average angle formed  
755 by the line segments that passed within its circular radius. We set the arrow lengths to be inversely  
756 proportional to the  $p$ -values of the Rayleigh tests at each vertex. Specifically, for each vertex we  
757 converted all of the angles of segments that passed within 2.4 units to unit vectors, and we set  
758 the arrow lengths at each vertex proportional to the length of the (circular) mean vector. We also  
759 indicated any significant results ( $p < 0.05$ , corrected using the Benjamani-Hochberg procedure) by  
760 coloring the arrows in blue (darker blue denotes a lower  $p$ -value, i.e., a longer mean vector); all  
761 tests with  $p \geq 0.05$  are displayed in gray and given a lower opacity value.

## 762 **Searchlight fMRI analyses**

763 In Figure 9, we present two analyses aimed at identifying brain regions whose responses (as par-  
764 ticipants viewed the video) exhibited a particular temporal structure. We developed a searchlight  
765 analysis wherein we constructed a  $5 \times 5 \times 5$  cube of voxels (following Chen et al., 2017) centered on  
766 each voxel in the brain, and for each of these cubes, computed the temporal correlation matrix of  
767 the voxel responses during video viewing. Specifically, for each of the 1976 volumes collected dur-  
768 ing video viewing, we correlated the activity patterns in the given cube with the activity patterns  
769 (in the same cube) collected during every other timepoint. This yielded a 1976 by 1976 correlation  
770 matrix for each cube. Note: participant 5's scan ended 75s early, and in Chen et al., 2017's publicly  
771 released dataset, their scan data was padded to match the length of the other participants'. For  
772 our searchlight analyses, we removed this padded data (i.e., the last 50 TRs), resulting in a 1925 by  
773 1925 correlation matrix for each cube in participant 5's brain.

774 Next, we constructed a series of "template" matrices: the first reflecting the timecourse of  
775 video's topic trajectory, and the others reflecting that of each participant's recall topic trajectory.  
776 To construct the video template, we computed the correlations between the topic proportions  
777 estimated for every pair of TRs (prior to segmenting the trajectory into discrete events; i.e., the  
778 correlation matrix shown in Figs. 2B and 9A). We constructed similar temporal correlation matrices  
779 for each participant's recall topic trajectory (Figs. 2D, S4). However, to correct for length differences

780 and potential non-linear transformations between viewing time and recall time, we first used  
781 dynamic time warping (Berndt and Clifford, 1994) to temporally align participants' recall topic  
782 trajectories with the video topic trajectory. An example correlation matrix before and after warping  
783 is shown in Fig. 9B. This yielded a 1976 by 1976 correlation matrix for the video template and for  
784 each participant's recall template.

785 The temporal structure of the video's content (as described by our model) is captured in the  
786 block-diagonal structure of the video's temporal correlation matrix (e.g., Figs. 2B, 9A), with time  
787 periods of thematic stability represented as dark blocks of varying sizes. Inspecting the video  
788 correlation matrix suggests that the video's semantic content is highly temporally specific (i.e.,  
789 the correlations between topic vectors from distant timepoints are almost entirely near-zero).  
790 By contrast, the activity patterns of individual (cubes of) voxels can encode relatively limited  
791 information on their own, and their activity frequently contributes to multiple separate functions  
792 (Freedman et al., 2001; Sigman and Dehaene, 2008; Charron and Koechlin, 2010; Rishel et al., 2013).  
793 By nature, these two attributes give rise to similarities in activity across large timescales that may  
794 not necessarily reflect a single task. To enable a more sensitive analysis of brain regions whose shifts  
795 in activity patterns mirrored shifts in the semantic content of the video or recalls, we restricted the  
796 temporal correlations we considered to timescale of semantic information captured by our model.  
797 Specifically, we isolated the upper triangle of the video correlation matrix and created a "proximal  
798 correlation mask" that included only diagonals from the upper triangle of the video correlation  
799 matrix up to the first that contained no positive correlations. Applying this mask to the full video  
800 correlation matrix was analogous to excluding diagonals beyond the corner of the largest diagonal  
801 block. In other words, the timescale of temporal correlations we considered corresponded to the  
802 longest period of thematic stability in the video, and by extension the longest expected period  
803 of thematic stability in participants' recalls and the longest period of stability we might expect  
804 to see in voxel activity arising from processing or encoding video content. Figure 9 shows this  
805 proximal correlation mask applied to the temporal correlation matrices for the video, an example  
806 participant's (warped) recall, and an example cube of voxels from our searchlight analyses.

807 To determine which (cubes of) voxel responses matched the video template, we correlated the

808 proximal diagonals from the upper triangle of the voxel correlation matrix for each cube with the  
809 proximal diagonals from video template matrix (Kriegeskorte et al., 2008). This yielded, for each  
810 participant, a voxelwise map of correlation values. We then performed a one-sample *t*-test on the  
811 distribution of (Fisher *z*-transformed) correlations at each voxel, across participants. This resulted  
812 in a value for each voxel (cube), describing how reliably its timecourse mirrored that of the video.

813 We further sought to ensure that our analysis identified regions where the activations' temporal  
814 structure specifically reflected that of the video, rather than regions whose activity was simply  
815 autocorrelated at a width similar to the video template's diagonal. To achieve this, we used a phase  
816 shift-based permutation procedure, wherein we circularly shifted the video's topic trajectory by  
817 a random number of timepoints, computed the resulting "null" video template, and re-ran the  
818 searchlight analysis, in full. (For each of the 100 permutations, the same random shift was used for  
819 all participants). We *z*-scored the observed (unshifted) result at each voxel against the distribution  
820 of permutation-derived "null" results, and estimated a *p*-value by computing the proportion of  
821 shifted results that yielded larger values. To create the map in Figure 9C, we thresholded out  
822 any voxels whose similarity to the unshifted video's structure fell below the 95<sup>th</sup> percentile of the  
823 permutation-derived similarity results.

824 We used an analogous procedure to identify which voxels' responses reflected the recall tem-  
825 plates. For each participant, we correlated the proximal diagonals from the upper triangle of the  
826 correlation matrix for each cube of voxels with the proximal diagonals from the upper triangle  
827 of their (time-warped) recall correlation matrix. As in the video template analysis, this yielded a  
828 voxelwise map of correlation coefficients per participant. However, whereas the video analysis  
829 compared every participant's responses to the same template, here the recall templates were unique  
830 for each participant. As in the analysis described above, we *t*-scored the (Fisher *z*-transformed)  
831 voxelwise correlations, and used the same permutation procedure we developed for the video  
832 responses to ensure specificity to the recall timeseries and assign significance values. To create the  
833 map in Figure 9D we again thresholded out any voxels whose correspondence values fell below  
834 the 95<sup>th</sup> percentile of the permutation-derived null distribution.

835 **References**

- 836 Atkinson, R. C. and Shiffrin, R. M. (1968). Human memory: A proposed system and its control  
837 processes. In Spence, K. W. and Spence, J. T., editors, *The psychology of learning and motivation*,  
838 volume 2, pages 89–105. Academic Press, New York.
- 839 Baldassano, C., Chen, J., Zadbood, A., Pillow, J. W., Hasson, U., and Norman, K. A. (2017).  
840 Discovering event structure in continuous narrative perception and memory. *Neuron*, 95(3):709–  
841 721.
- 842 Baldassano, C., Hasson, U., and Norman, K. A. (2018). Representation of real-world event schemas  
843 during narrative perception. *Journal of Neuroscience*, 38(45):9689–9699.
- 844 Berndt, D. J. and Clifford, J. (1994). Using dynamic time warping to find patterns in time series. In  
845 *KDD workshop*, volume 10, pages 359–370.
- 846 Blei, D. M. and Lafferty, J. D. (2006). Dynamic topic models. In *Proceedings of the 23rd International  
847 Conference on Machine Learning*, ICML '06, pages 113–120, New York, NY, US. ACM.
- 848 Blei, D. M., Ng, A. Y., and Jordan, M. I. (2003). Latent dirichlet allocation. *Journal of Machine  
849 Learning Research*, 3:993 – 1022.
- 850 Brunec, I. K., Moscovitch, M. M., and Barense, M. D. (2018). Boundaries shape cognitive represen-  
851 tations of spaces and events. *Trends in Cognitive Sciences*, 22(7):637–650.
- 852 Bylinskii, Z., Isola, P., Bainbridge, C., Torralba, A., and Oliva, A. (2015). Intrinsic and extrinsic  
853 effects on image memorability. *Vision Research*, 116:165–178.
- 854 Capota, M., Turek, J., Chen, P.-H., Zhu, X., Manning, J. R., Sundaram, N., Keller, B., Wang, Y., and  
855 Shin, Y. S. (2017). Brain imaging analysis kit.
- 856 Cer, D., Yang, Y., Kong, S. Y., Hua, N., Limtiaco, N., John, R. S., Constant, N., Guajardo-Cespedes,  
857 M., Yuan, S., Tar, C., Sung, Y.-H., Strope, B., and Kurzweil, R. (2018). Universal sentence encoder.  
858 *arXiv*, 1803.11175.

- 859 Charron, S. and Koechlin, E. (2010). Divided representations of current goals in the human frontal  
860 lobes. *Science*, 328(5976):360–363.
- 861 Chen, J., Leong, Y. C., Honey, C. J., Yong, C. H., Norman, K. A., and Hasson, U. (2017). Shared  
862 memories reveal shared structure in neural activity across individuals. *Nature Neuroscience*,  
863 20(1):115.
- 864 Chun, M. and Turk-Browne, N. (2007). Interactions between attention and memory. *Current opinion*  
865 in *neurobiology*, 17(2):177–184.
- 866 Clewett, D. and Davachi, L. (2017). The ebb and flow of experience determines the temporal  
867 structure of memory. *Curr Opin Behav Sci*, 17:186–193.
- 868 Dobrushin, R. L. (1970). Prescribing a system of random variables by conditional distributions.  
869 *Theory of Probability & Its Applications*, 15(3):458–486.
- 870 DuBrow, S. and Davachi, L. (2013). The influence of contextual boundaries on memory for the  
871 sequential order of events. *Journal of Experimental Psychology: General*, 142(4):1277–1286.
- 872 Ezzyat, Y. and Davachi, L. (2011). What constitutes an episode in episodic memory? *Psychological*  
873 *Science*, 22(2):243–252.
- 874 Fisher, R. A. (1925). *Statistical Methods for Research Workers*. Oliver and Boyd.
- 875 Freedman, D., Riesenhuber, M., Poggio, T., and Miller, E. (2001). Categorical representation of  
876 visual stimuli in the primate prefrontal cortex. *Science*, 291(5502):312–316.
- 877 Friendly, M., Franklin, P. E., Hoffman, D., and Rubin, D. C. (1982). The Toronto Word Pool:  
878 Norms for imagery, concreteness, orthographic variables, and grammatical usage for 1,080  
879 words. *Behavior Research Methods and Instrumentation*, 14:375–399.
- 880 Hasson, U., Chen, J., and Honey, C. J. (2015). Hierarchical process memory: memory as an integral  
881 component of information processing. *Trends in Cognitive Science*, 19(6):304–315.

- 882 Hasson, U., Yang, E., Vallines, I., Heeger, D. J., and Rubin, N. (2008). A hierarchy of temporal  
883 receptive windows in human cortex. *Journal of Neuroscience*, 28(10):2539–2550.
- 884 Heusser, A. C., Ezzyat, Y., Shiff, I., and Davachi, L. (2018a). Perceptual boundaries cause mnemonic  
885 trade-offs between local boundary processing and across-trial associative binding. *Journal of  
886 Experimental Psychology Learning, Memory, and Cognition*, 44(7):1075–1090.
- 887 Heusser, A. C., Fitzpatrick, P. C., Field, C. E., Ziman, K., and Manning, J. R. (2017). Quail: a  
888 Python toolbox for analyzing and plotting free recall data. *The Journal of Open Source Software*,  
889 10.21105/joss.00424.
- 890 Heusser, A. C., Ziman, K., Owen, L. L. W., and Manning, J. R. (2018b). HyperTools: a Python  
891 toolbox for gaining geometric insights into high-dimensional data. *Journal of Machine Learning  
892 Research*, 18(152):1–6.
- 893 Howard, M. W. and Kahana, M. J. (2002). A distributed representation of temporal context. *Journal  
894 of Mathematical Psychology*, 46:269–299.
- 895 Howard, M. W., MacDonald, C. J., Tiganj, Z., Shankar, K. H., Du, Q., Hasselmo, M. E., and H., E.  
896 (2014). A unified mathematical framework for coding time, space, and sequences in the medial  
897 temporal lobe. *Journal of Neuroscience*, 34(13):4692–4707.
- 898 Howard, M. W., Viskontas, I. V., Shankar, K. H., and Fried, I. (2012). Ensembles of human MTL  
899 neurons “jump back in time” in response to a repeated stimulus. *Hippocampus*, 22:1833–1847.
- 900 Huk, A., Bonnen, K., and He, B. J. (2018). Beyond trial-based paradigms: continuous behavior, on-  
901 going neural activity, and naturalistic stimuli. *Journal of Neuroscience*, 10.1523/JNEUROSCI.1920-  
902 17.2018.
- 903 Kahana, M. J. (1996). Associative retrieval processes in free recall. *Memory & Cognition*, 24:103–109.
- 904 Kelly, S., Lloyd, D., Nurmikko, T., and Roberts, N. (2007). Retrieving autobiographical memories  
905 of painful events activates the anterior cingulate cortex and inferior frontal gyrus. *THe Journal of  
906 Pain*, 8(4):307–314.

- 907 Koriat, A. and Goldsmith, M. (1994). Memory in naturalistic and laboratory contexts: distin-  
908 guishing accuracy-oriented and quantity-oriented approaches to memory assessment. *Journal of*  
909 *Experimental Psychology: General*, 123(3):297–315.
- 910 Kriegeskorte, N., Mur, M., and Bandettini, P. (2008). Representational similarity analysis – con-  
911 necting the branches of systems neuroscience. *Frontiers in Systems Neuroscience*, 2:1 – 28.
- 912 Landauer, T. K., Foltz, P. W., and Laham, D. (1998). Introduction to latent semantic analysis.  
913 *Discourse Processes*, 25:259–284.
- 914 Lerner, Y., Honey, C. J., Silbert, L. J., and Hasson, U. (2011). Topographic mapping of a hierarchy  
915 of temporal receptive windows using a narrated story. *Journal of Neuroscience*, 31(8):2906–2915.
- 916 Manning, J. R. (2019). Episodic memory: mental time travel or a quantum 'memory wave' function?  
917 *PsyArXiv*, doi:10.31234/osf.io/6zjwb.
- 918 Manning, J. R., Norman, K. A., and Kahana, M. J. (2015). The role of context in episodic memory.  
919 In Gazzaniga, M., editor, *The Cognitive Neurosciences, Fifth edition*, pages 557–566. MIT Press.
- 920 Manning, J. R., Polyn, S. M., Baltuch, G., Litt, B., and Kahana, M. J. (2011). Oscillatory patterns  
921 in temporal lobe reveal context reinstatement during memory search. *Proceedings of the National*  
922 *Academy of Sciences, USA*, 108(31):12893–12897.
- 923 McInnes, L., Healy, J., and Melville, J. (2018). UMAP: Uniform manifold approximation and  
924 projection for dimension reduction. *arXiv*, 1802(03426).
- 925 Medford, N. and Critchley, H. D. (2010). Conjoint activity of anterior insular and anterior cingulate  
926 cortex: awareness and response. *Brain Structure and Function*, 214(5-6):535–549.
- 927 Menon, V. and Uddin, L. Q. (2010). Saliency, switching, attention and control: a network model of  
928 insula function. *Brain Structure and Function*, 214(5-6):655–667.
- 929 Mikolov, T., Chen, K., Corrado, G., and Dean, J. (2013). Efficient estimation of word representations  
930 in vector space. *arXiv*, 1301.3781.

- 931 Mueller, A., Fillion-Robin, J.-C., Boidol, R., Tian, F., Nechifor, P., yoonsubKim, Peter, Rampin, R.,  
932 Corvellec, M., Medina, J., Dai, Y., Petrushev, B., Langner, K. M., Hong, Alessio, Ozsvald, I.,  
933 vkolmakov, Jones, T., Bailey, E., Rho, V., IgorAPM, Roy, D., May, C., foobuzz, Piyush, Seong,  
934 L. K., Goey, J. V., Smith, J. S., Gus, and Mai, F. (2018). WordCloud 1.5.0: a little word cloud  
935 generator in Python. *Zenodo*, <https://zenodo.org/record/1322068#.W4tPKZNKh24>.
- 936 Murdock, B. B. (1962). The serial position effect of free recall. *Journal of Experimental Psychology*,  
937 64:482–488.
- 938 Paller, K. A. and Wagner, A. D. (2002). Observing the transformation of experience into memory.  
939 *Trends in Cognitive Sciences*, 6(2):93–102.
- 940 Pedregosa, F., Varoquaux, G., Gramfort, A., Michel, V., Thirion, B., Grisel, O., Blondel, M., Pretten-  
941 hofer, P., Weiss, R., Dubourg, V., Vanderplas, J., Passos, A., Cournapeau, D., Brucher, M., Perrot,  
942 M., and Duchesnay, E. (2011). Scikit-learn: Machine learning in Python. *Journal of Machine  
943 Learning Research*, 12:2825–2830.
- 944 Polyn, S. M., Norman, K. A., and Kahana, M. J. (2009). A context maintenance and retrieval model  
945 of organizational processes in free recall. *Psychological Review*, 116(1):129–156.
- 946 Postman, L. and Phillips, L. W. (1965). Short-term temporal changes in free recall. *Quarterly Journal  
947 of Experimental Psychology*, 17:132–138.
- 948 Rabiner, L. (1989). A tutorial on Hidden Markov Models and selected applications in speech  
949 recognition. *Proceedings of the IEEE*, 77(2):257–286.
- 950 Radvansky, G. A. and Zacks, J. M. (2017). Event boundaries in memory and cognition. *Curr Opin  
951 Behav Sci*, 17:133–140.
- 952 Ramdas, A., Trillos, N., and Cuturi, M. (2017). On wasserstein two-sample testing and related  
953 families of nonparametric tests. *Entropy*, 19(2):47.
- 954 Ranganath, C. and Ritchey, M. (2012). Two cortical systems for memory-guided behavior. *Nature  
955 Reviews Neuroscience*, 13:713 – 726.

- 956 Rishel, C. A., Huang, G., and Freedman, D. J. (2013). Independent category and spatial encoding  
957 in parietal cortex. *Neuron*, 77(5):969–979.
- 958 Sigman, M. and Dehaene, S. (2008). Brain mechanisms of serial and parallel processing during  
959 dual-task performance. *Journal of Neuroscience*, 28(30):7585–7589.
- 960 Simony, E., Honey, C. J., Chen, J., and Hasson, U. (2016). Uncovering stimulus-locked network  
961 dynamics during narrative comprehension. *Nature Communications*, 7(12141):1–13.
- 962 Stark, S. M., Yassa, M. A., and Stark, C. E. L. (2010). Individual differences in spatial pattern  
963 separation performance associated with healthy aging in humans. *Learning & Memory*, 17(6):284–  
964 288.
- 965 Steyvers, M., Shiffrin, R. M., and Nelson, D. L. (2004). Word association spaces for predicting  
966 semantic similarity effects in episodic memory. In Healy, A. F., editor, *Cognitive Psychology and*  
967 *its Applications: Festschrift in Honor of Lyle Bourne, Walter Kintsch, and Thomas Landauer*. American  
968 Psychological Association, Washington, DC.
- 969 Tomrary, A. and Davachi, L. (2017). Consolidation promotes the emergence of representational  
970 overlap in the hippocampus and medial prefrontal cortex. *Neuron*, 96(1):228–241.
- 971 Tyng, C. M., Amin, H. U., Saad, M. N. M., and S, M. A. (2017). The influences of emotion on  
972 learning and memory. *Frontiers in psychology*, 8:1454.
- 973 Waskom, M., Botvinnik, O., Okane, D., Hobson, P., David, Halchenko, Y., Lukauskas, S., Cole, J. B.,  
974 Warmenhoven, J., de Ruiter, J., Hoyer, S., Vanderplas, J., Villalba, S., Kunter, G., Quintero, E.,  
975 Martin, M., Miles, A., Meyer, K., Augspurger, T., Yarkoni, T., Bachant, P., Williams, M., Evans,  
976 C., Fitzgerald, C., Brian, Wehner, D., Hitz, G., Ziegler, E., Qalieh, A., and Lee, A. (2016). Seaborn:  
977 v0.7.1.
- 978 Welch, G. B. and Burnett, C. T. (1924). Is primacy a factor in association-formation. *American Journal*  
979 *of Psychology*, 35:396–401.

- 980 Yarkoni, T., Poldrack, R. A., Nichols, T. E., Van Essen, D. C., and Wager, T. D. (2011). Large-scale  
981 automated synthesis of human functional neuroimaging data. *Nature Methods*, 8(8):665.
- 982 Yassa, M. A., Lacy, J. W., Stark, S. M., Albert, M. S., Gallagher, M., and Stark, C. E. L. (2011). Pattern  
983 separation deficits associated with increased hippocampal ca3 and dentate gyrus activity in  
984 nondemented older adults. *Hippocampus*, 21(9):968–979.
- 985 Yassa, M. A. and Stark, C. E. L. (2011). Pattern separation in the hippocampus. *Trends In Neuro-*  
986 *sciences*, 34(10):515–525.
- 987 Yonelinas, A. P. (2002). The nature of recollection and familiarity: A review of 30 years of research.  
988 *Journal of Memory and Language*, 46:441–517.
- 989 Yonelinas, A. P., Kroll, N. E., Quamme, J. R., Lazzara, M. M., Sauvé, M. J., Widaman, K. F., and  
990 Knight, R. T. (2002). Effects of extensive temporal lobe damage or mild hypoxia on recollection  
991 and familiarity. *Nature Neuroscience*, 5(11):1236–41.
- 992 Zacks, J. M., Speer, N. K., Swallow, K. M., Braver, T. S., and Reynolds, J. R. (2007). Event perception:  
993 a mind-brain perspective. *Psychological Bulletin*, 133:273–293.
- 994 Zadbood, A., Chen, J., Leong, Y. C., Norman, K. A., and Hasson, U. (2017). How we transmit  
995 memories to other brains: Constructing shared neural representations via communication. *Cereb*  
996 *Cortex*, 27(10):4988–5000.
- 997 Zwaan, R. A. and Radvansky, G. A. (1998). Situation models in language comprehension and  
998 memory. *Psychological Bulletin*, 123(2):162 – 185.

999 **Supporting information**

1000 Supporting information is available in the online version of the paper.

1001 **Acknowledgements**

1002 We thank Luke Chang, Janice Chen, Chris Honey, Lucy Owen, Emily Whitaker, and Kirsten Ziman  
1003 for feedback and scientific discussions. We also thank Janice Chen, Yuan Chang Leong, Kenneth  
1004 Norman, and Uri Hasson for sharing the data used in our study. Our work was supported in part  
1005 by NSF EPSCoR Award Number 1632738. The content is solely the responsibility of the authors  
1006 and does not necessarily represent the official views of our supporting organizations.

1007 **Author contributions**

1008 Conceptualization: A.C.H. and J.R.M.; Methodology: A.C.H., P.C.F. and J.R.M.; Software: A.C.H.,  
1009 P.C.F. and J.R.M.; Analysis: A.C.H., P.C.F. and J.R.M.; Writing, Reviewing, and Editing: A.C.H.,  
1010 P.C.F. and J.R.M.; Supervision: J.R.M.

1011 **Author information**

1012 The authors declare no competing financial interests. Correspondence and requests for materials  
1013 should be addressed to J.R.M. (jeremy.r.manning@dartmouth.edu).